-ELECTRONIC SUPPORTING INFORMATION (ESI)-

Mechanism of Halogen Exchange in ATRP

*Chi-How Peng, Jing Kong, Florian Seeliger and Krzysztof Matyjaszewski**

Department of Chemistry, Carnegie Mellon University, Pittsburgh, PA 15213, USA

* Corresponding author: E-mail: km3b@andrew.cmu.edu

Table of contents

Experimental Section

Materials. Methyl bromoacetate (MBrA, 97%, Aldrich), methyl 2-bromopropionate (MBrP, 98%, Aldrich), methyl 2-bromoisobutyrate (MBriB, 99%, Aldrich), ethyl 2-bromoisobutyrate (EtBriB, 99%, Aldrich), bromoacetonitrile (BrAN, 97%, Aldrich), 2-bromopropionitrile (BrPN, 97%, Aldrich), chloroacetonitrile (ClAN, 99%, Aldrich), benzyl bromide (BnBr, 98%, Aldrich), 1-(bromoethyl)benzene (PEBr, 97%, Aldrich), and 1-(chloroethyl)benzene (PECl, Aldrich) were distilled prior to use. Tris(2-pyridylmethyl)amine (TPMA, ATRP Solutions), *N*,*N*,*N*′,*N*″,*N*″-pentamethyldiethylenetriamine (PMDETA, 99%, Aldrich), 2,2′-Bipyridine (bpy, ≧99%, Sigma-Aldrich), copper(I) chloride (CuCl, ≧99%, Aldrich), copper(II) chloride ($CuCl_2$, ≧99%, Aldrich), Tetrabutylammonium chloride (NBu_4Cl, ≧97%, Aldrich), 2,2,6,6-tetramethylpiperidinyl-1-oxy (TEMPO, 99%, Aldrich), and acetonitrile (MeCN, HPLC-grade, Fisher) were used as received.

Measurements of Rate Constants for the Radical Pathway (Atom Transfer) (k_{act}). The activation rate constants (k_{act}) were determined by following the reactions of copper(I) chloride, ligands, initiators, and TEMPO in MeCN at 22°C using the time-dependent $Cu^{(II)}(L)X_2$ concentration measured by UV-vis-NIR spectroscopy obtained on a Varian Cary 5000 UV-Vis-NIR spectrophotometer. The time-dependent $Cu^{(II)}(L)X_2$ concentration was fitted by single exponential $y = A[1-\exp(-k_{obs}t)]+C$ to estimate the value of k_{obs}, which was then converted to k_{act} by $k_{act} = k_{obs}/[\text{initiator}]$. A specific example showing the measurement of k_{act} for $Cu^{(I)}(bpy)_2Cl$ with MBrP is provided in Figure 1. Nitrogen bubbled MeCN solutions of copper(I) chloride (3.64×10^{-2} mol L^{-1}, 0.30 mL), bpy (6.59×10^{-2} mol L^{-1}, 0.33 mL),

TEMPO (3.20×10^{-1} mol L^{-1}, 0.34 mL), and MeCN (2.30 mL) were injected into a nitrogen purged Schlenk flask, which was capped by a designed quartz cuvette. The initiator, MBrP (2.99×10^{-1} mol L^{-1}, 0.73 mL), was added into the flask via syringe to start the reaction.

Measurements of Rate Constants for an Ionic Pathway (Halide Exchange) (k_{ionic}). The rate constants of the ionic pathway (k_{ionic}) were estimated from the slope of second order kinetic plots of the conversion from alkyl bromide to alkyl chloride followed by ^{1}H NMR spectra obtained on a Bruker Avance 300 MHz NMR spectrometer at 27^{o}C. A specific example, measuring k_{ionic} for the reaction of $Cu^{(II)}(bpy)_2Cl_2$ with PEBr is shown in Figure 4. Nitrogen bubbled MeCN-d_3 solutions of copper(II) chloride (1.17×10^{-2} mol L^{-1}, 0.25 mL) and bpy (2.30×10^{-2} mol L^{-1}, 0.25 mL) were injected into a nitrogen purged NMR tube which was sealed by a rubber stopper. The initiator, PEBr in MeCN-d_3 (1.35×10^{-1} mol L^{-1}, 0.02 mL), was added into the tube via syringe to start the reaction.

Measurements of Rate Constants for Halogen Exchange (k_{HE}). The method used to measure the rate constants of halogen exchange (k_{HE}) is the same as that used to estimate k_{ionic}. A specific example of determining the k_{HE} for reaction between $Cu^{(I)}(bpy)_2Cl$ and MBrA is shown in Figure 6. Nitrogen bubbled MeCN-d_3 solutions of copper(I) chloride (7.42×10^{-2} mol L^{-1}, 0.12 mL), bpy (1.28×10^{-1} mol L^{-1}, 0.13 mL), and MeCN-d_3 (0.1 mL) were injected into a nitrogen purged NMR tube which was sealed by a rubber stopper. The MBrA MeCN-d_3 solution (1.62×10^{-1} mol L^{-1}, 0.05 mL), was added into the tube via syringe to start the reaction.

^{1}H NMR spectra of initiators

Acetonitrile-d_3 (MeCN-d_3) is the solvent used for all ^{1}H NMR spectrum and the solvent peak at 1.94 ppm was used for the calibration.

MBrA (Blue) and MClA (Red)

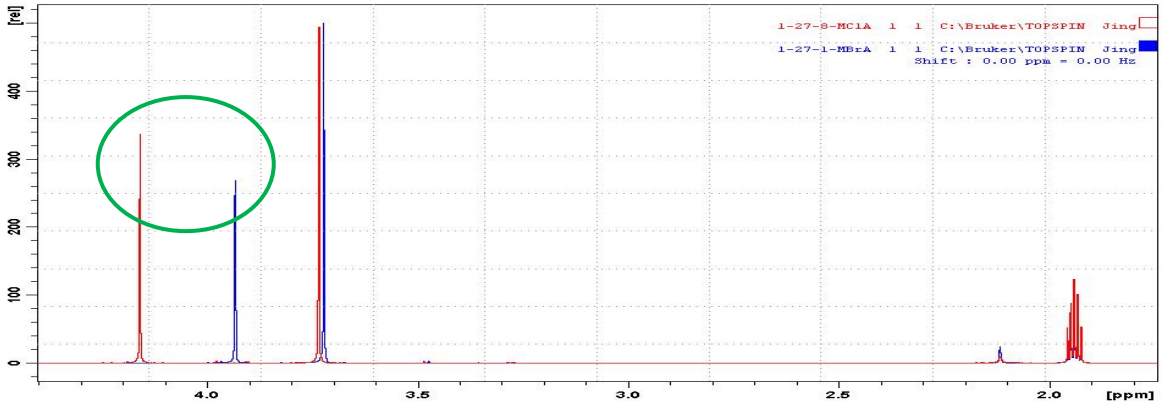

BnBr (Red) and BnCl (Blue)

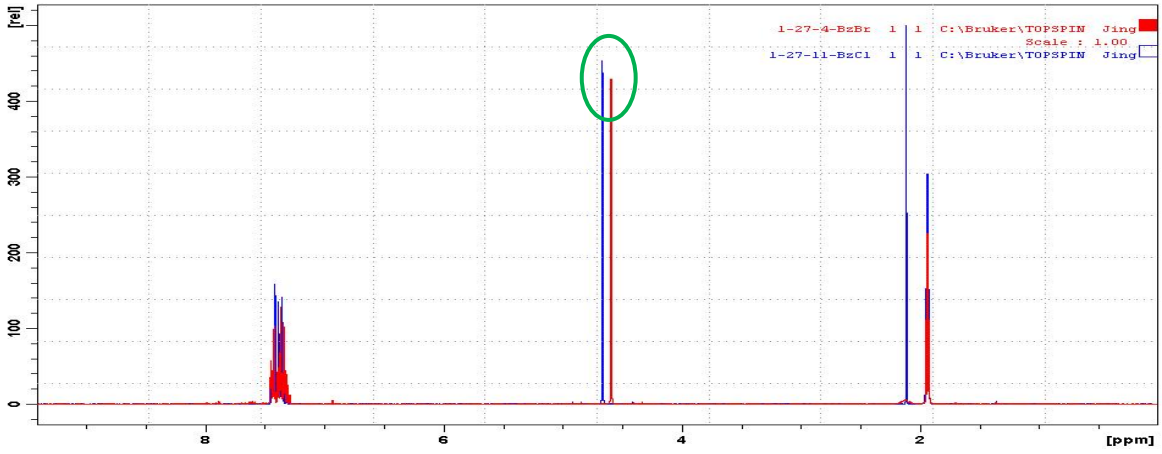

BrAN (Red) and ClAN (Blue)

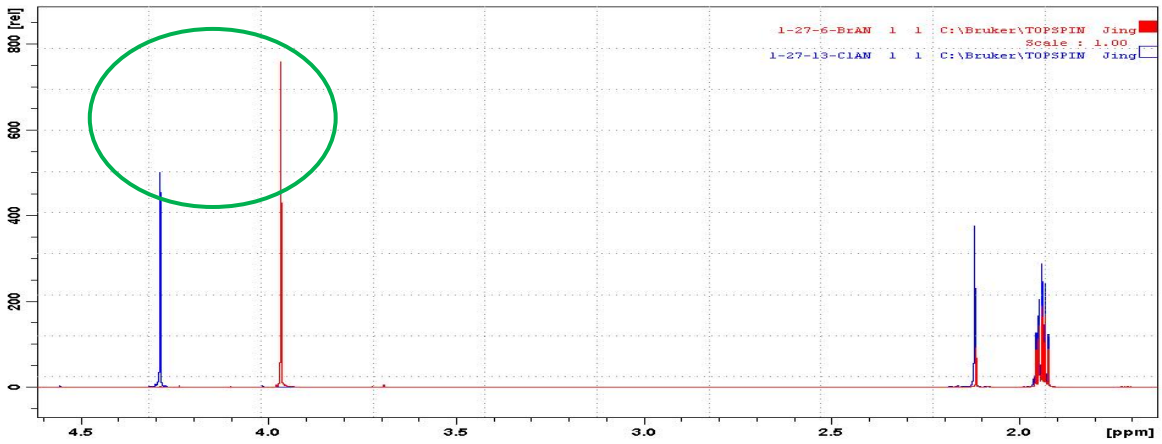

MBrP (Blue) and MClP (Red)

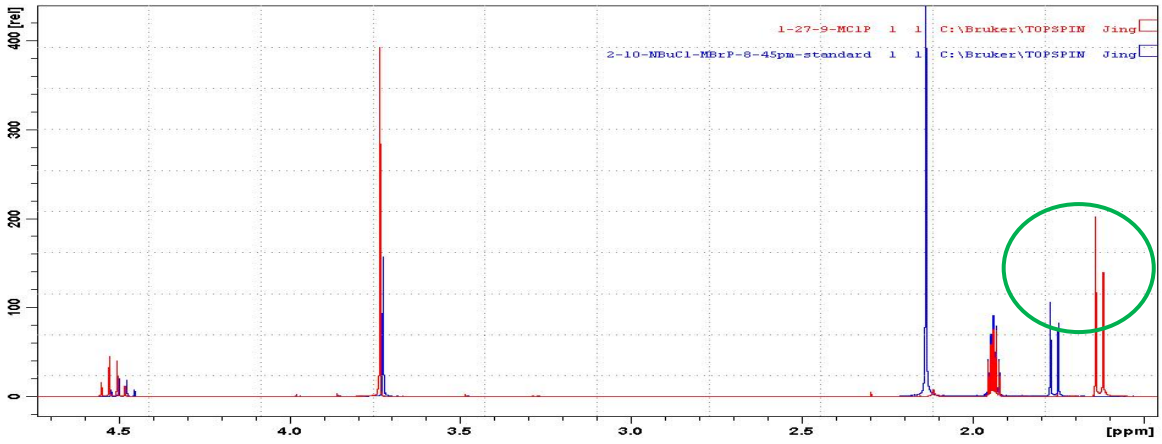

PEBr (Red) and PECl (Blue)

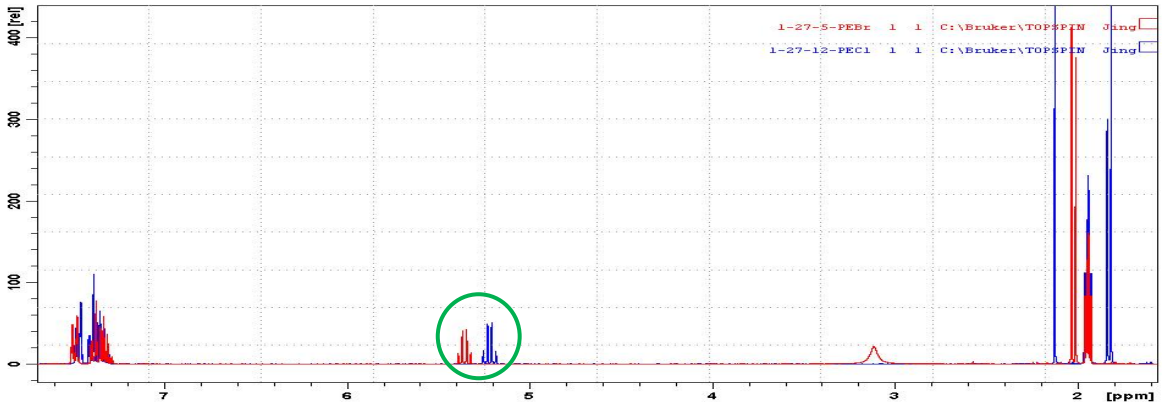

BrPN (Blue) and ClPN (Red)

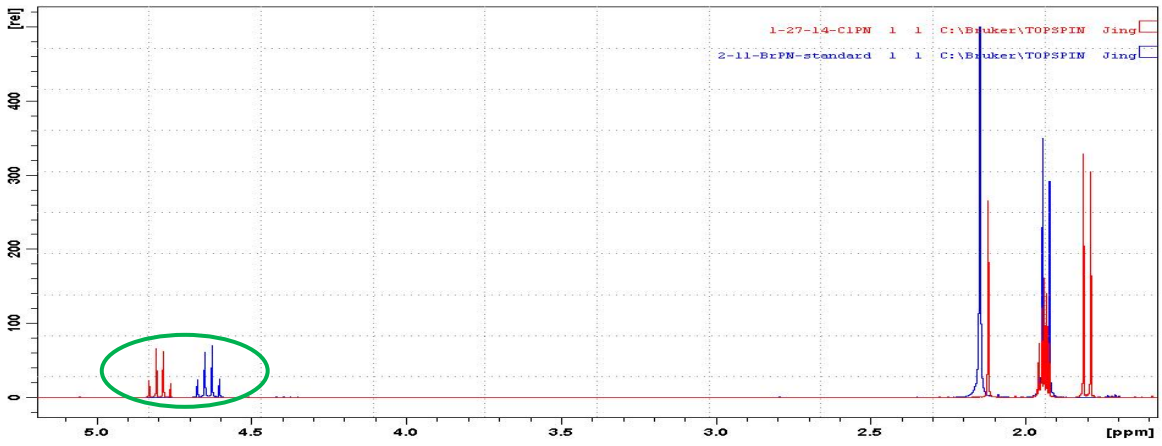

MBriB (Red) and MCliB (Blue)

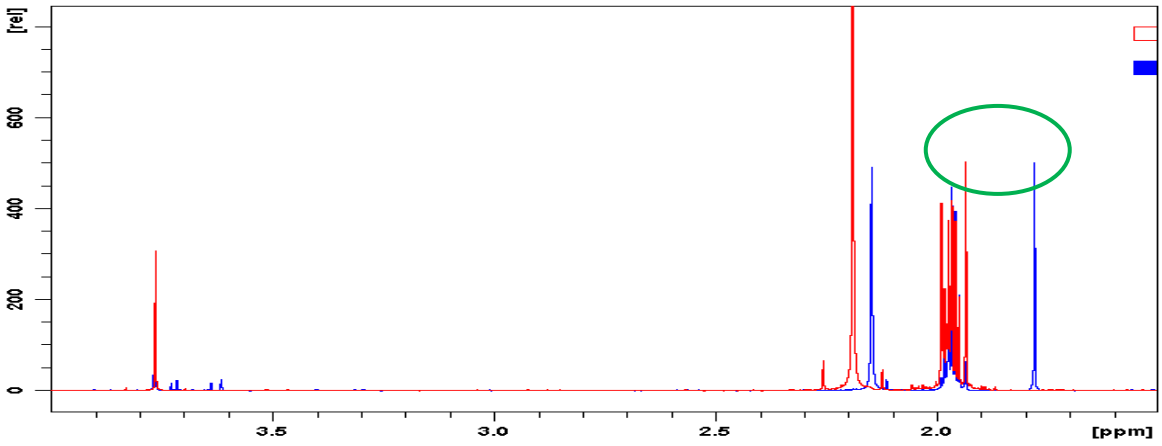

Measurements of activation rate constants (k_{act}) for selected initiators with Cu catalysts

Activation rate constants were estimated by UV-vis-NIR spectroscopy by following the absorbance at the λ_{max} of the formed $Cu^{(II)}$ complexes (740nm for $Cu^{(II)}(bpy)_2X_2$ and $Cu^{(II)}(PMDETA)X_2$; 950nm for $Cu^{(II)}(TPMA)X_2$). The single exponential equation, $y = A[1-\exp(-k_{obs}t)]+C$, was used to fit the observed time-dependent $Cu^{(II)}$ absorbance. The constant of k_{obs} can be converted to k_{act} by $k_{act} = k_{obs}/[\text{alkyl halide}]$ in the presence of a large excess of alkyl halide.

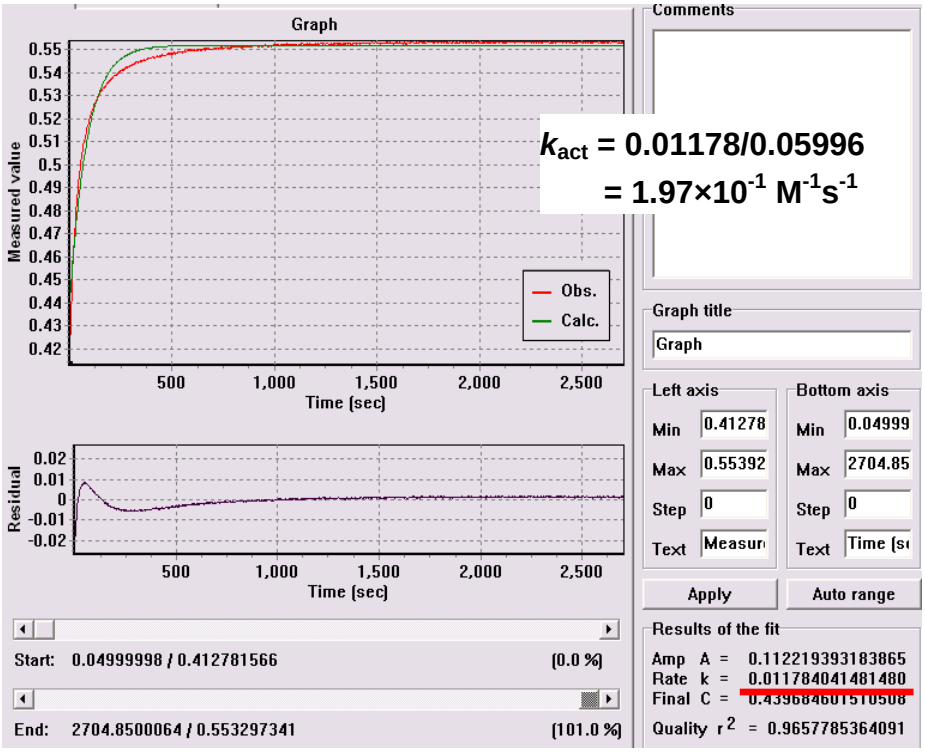

Figure SI1. Measurement of the activation rate constant for $Cu^{(I)}Cl$ species in MeCN at 27 ^{o}C. $[CuCl]_o/[TPMA]_o/[PECl]_o$ = 2.74mM/2.74mM/59.96mM.

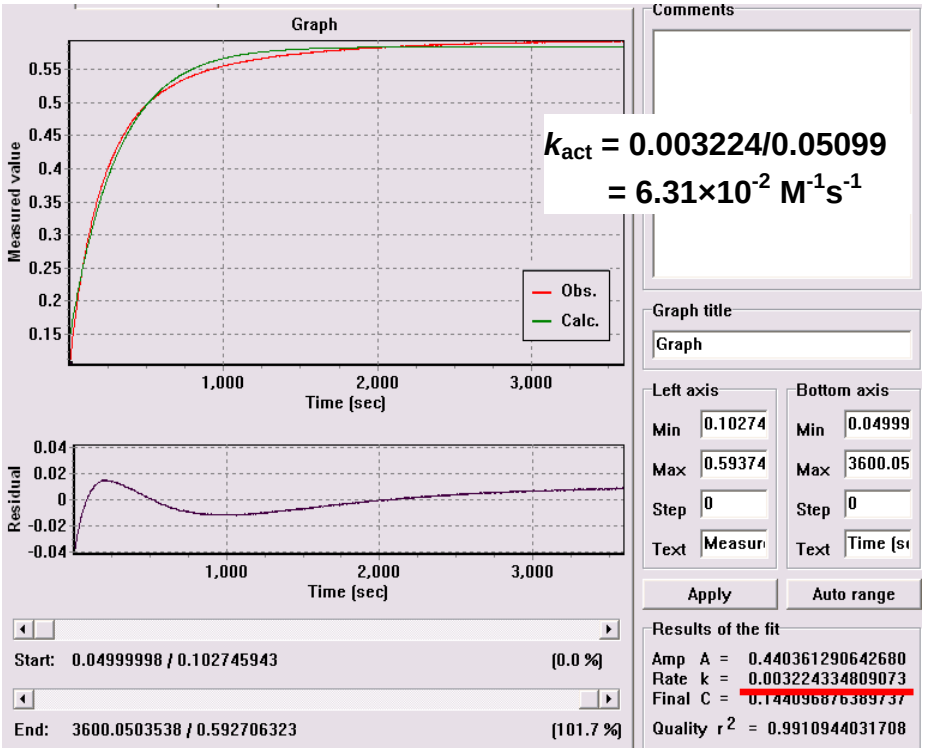

Figure SI2. Measurement of the activation rate constant for Cu$^{(I)}$Cl species in MeCN at 27 ^{o}C. $[CuCl]_o/[PMDETA]_o/[ClAN]_o$ = 2.83mM/2.83mM/50.99mM.

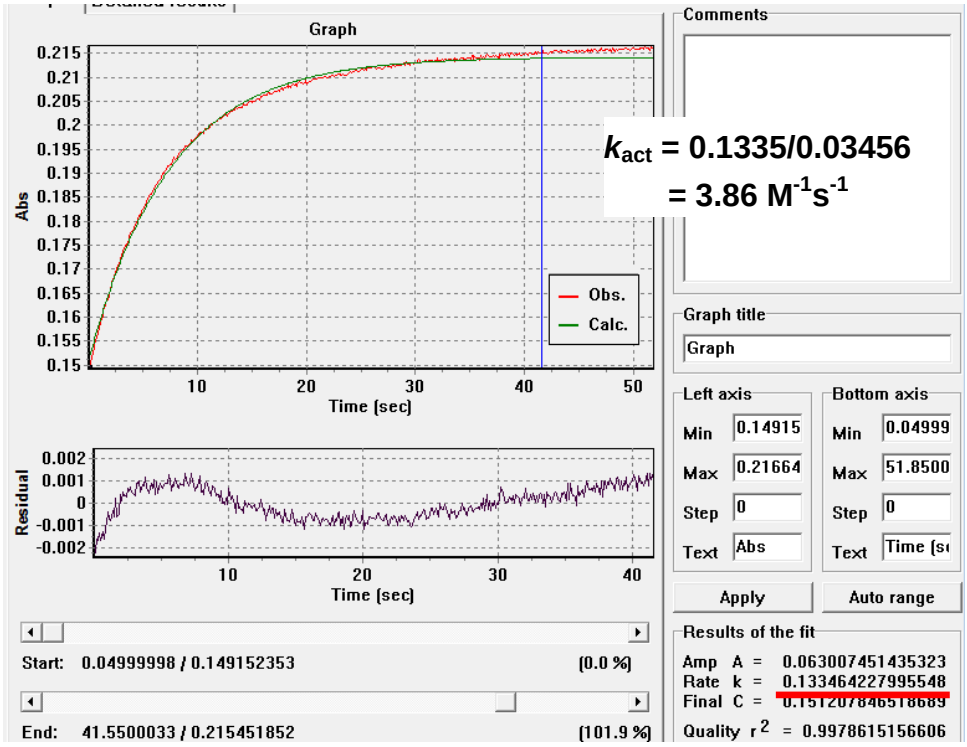

Figure SI3. Measurement of the activation rate constant for Cu$^{(I)}$Cl species in MeCN at 27 ^{o}C. $[CuCl]_o/[PMDETA]_o/[BrAN]_o$ = 1.11mM/1.11mM/34.56mM.

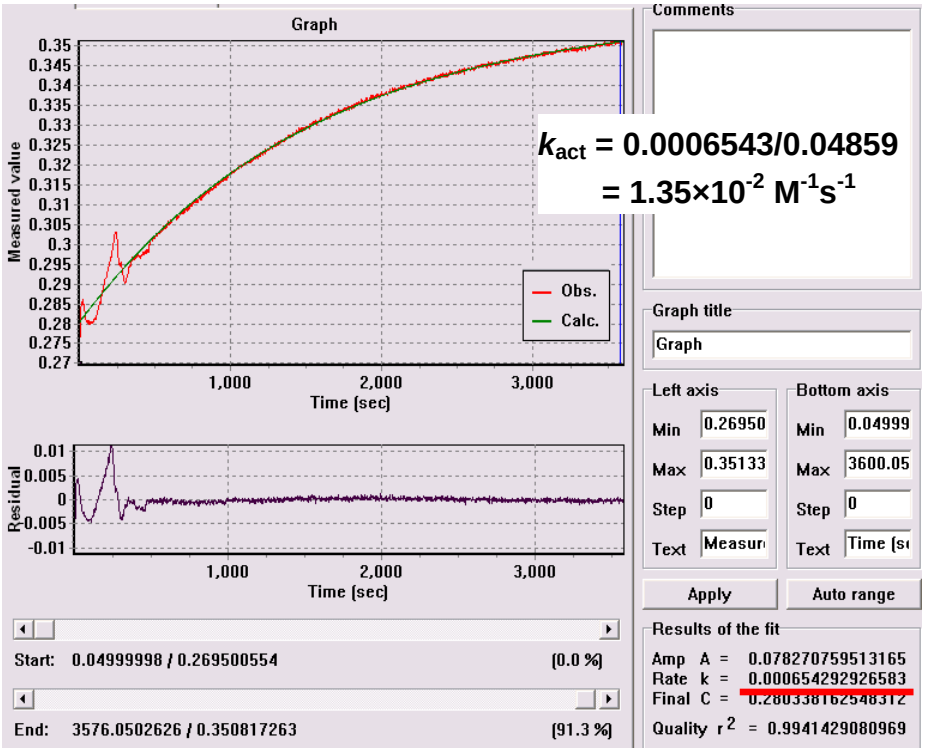

Figure SI4. Measurement of the activation rate constant for Cu$^{(I)}$Cl species in MeCN at 27 ^{o}C. $[CuCl]_o/[PMDETA]_o/[MBrA]_o$ = 2.55mM/2.56mM/48.59mM.

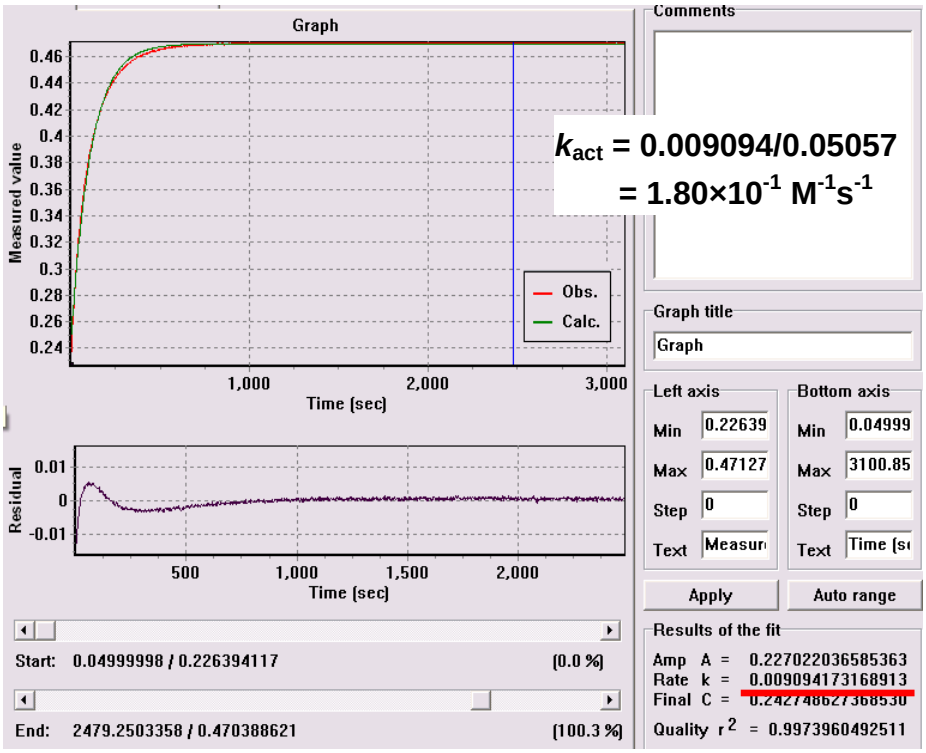

Figure SI5. Measurement of the activation rate constant for Cu$^{(I)}$Cl species in MeCN at 27 ^{o}C. $[CuCl]_o/[PMDETA]_o/[MBrP]_o$ = 2.55mM/2.56mM/50.57mM.

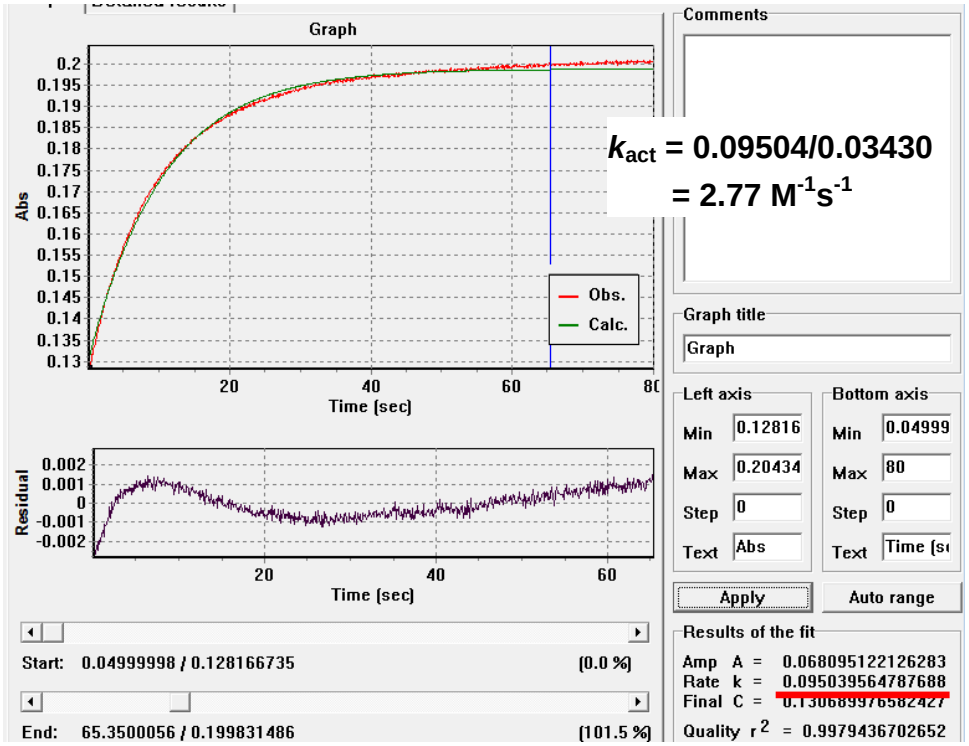

Figure SI6. Measurement of the activation rate constant for $Cu^{(I)}Cl$ species in MeCN at 27 °C. $[CuCl]_o/[PMDETA]_o/[MBriB]_o$ = 1.09mM/1.09mM/34.30mM.

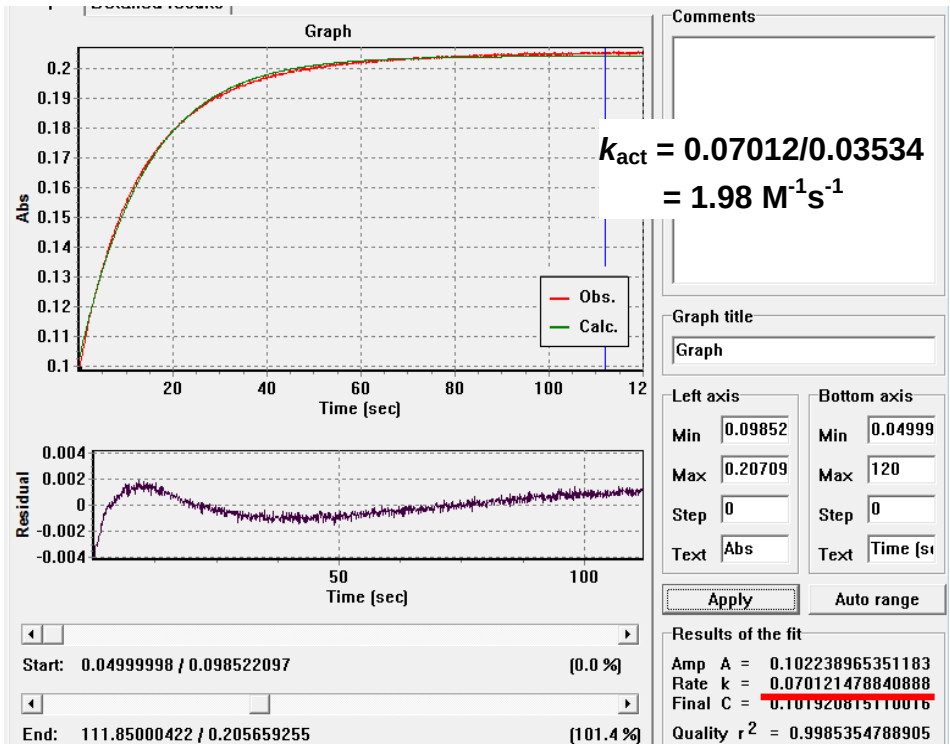

Figure SI7. Measurement of the activation rate constant for $Cu^{(I)}Cl$ species in MeCN at 27 °C. $[CuCl]_o/[PMDETA]_o/[EtBriB]_o$ = 1.09mM/1.09mM/35.34mM.

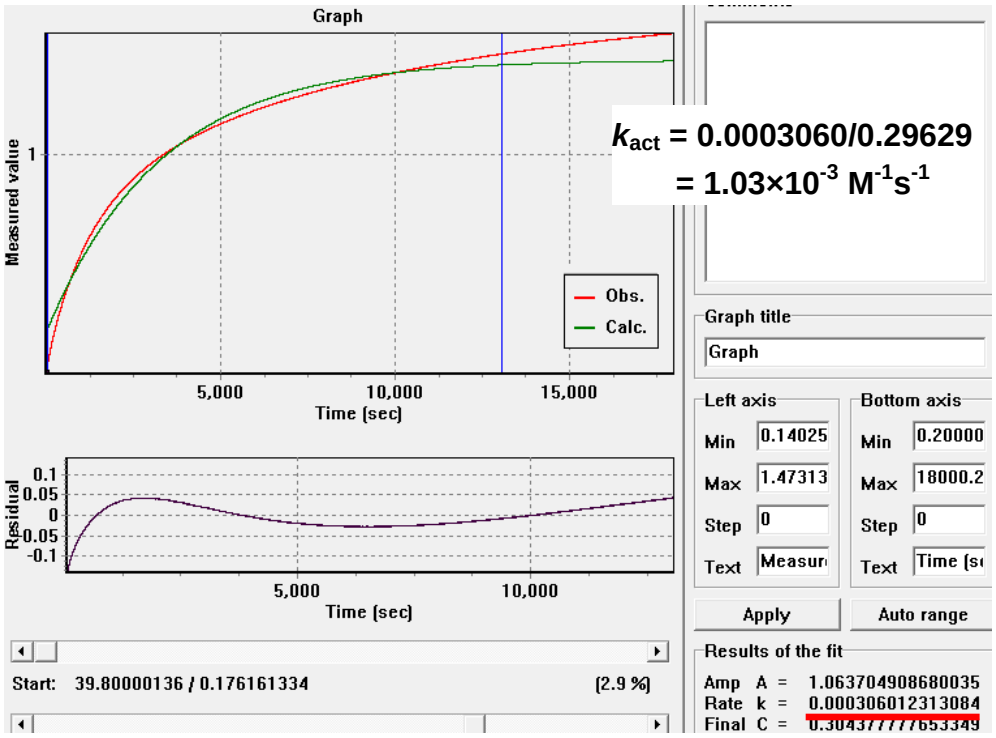

Figure SI8. Measurement of the activation rate constant for Cu$^{(I)}$Cl species in MeCN at 27 ^{o}C. $[CuCl]_o/[bpy]_o/[BnBr]_o$ = 9.70mM/19.50mM/296.29mM.

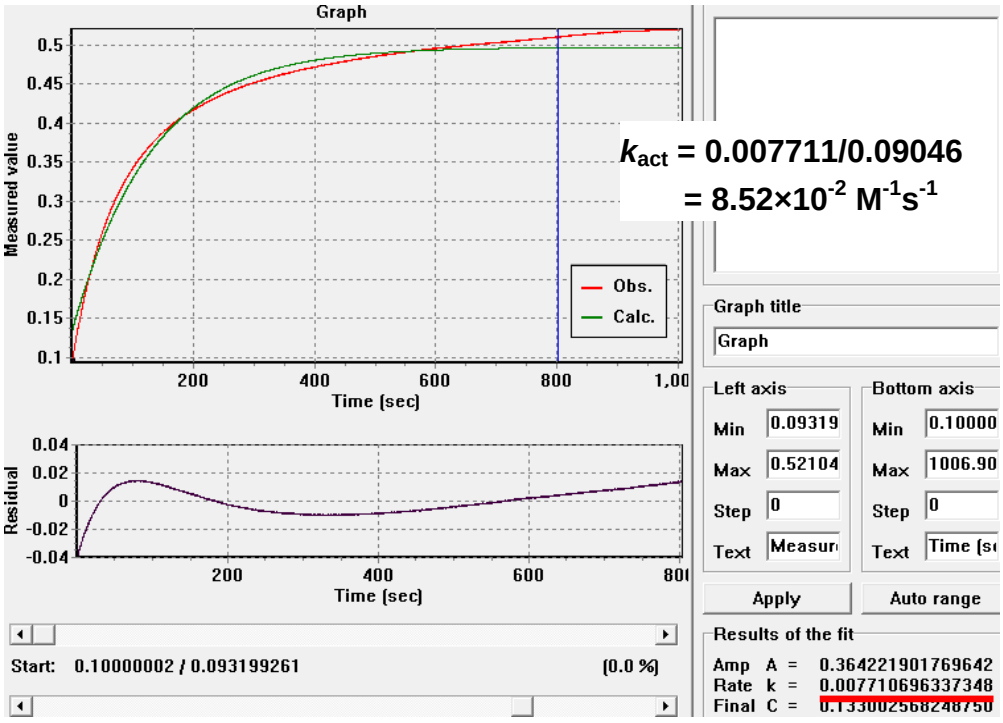

Figure SI9. Measurement of the activation rate constant for Cu$^{(I)}$Cl species in MeCN at 27 ^{o}C. $[CuCl]_o/[bpy]_o/[BrAN]_o$ = 4.49mM/9.00mM/90.46mM.

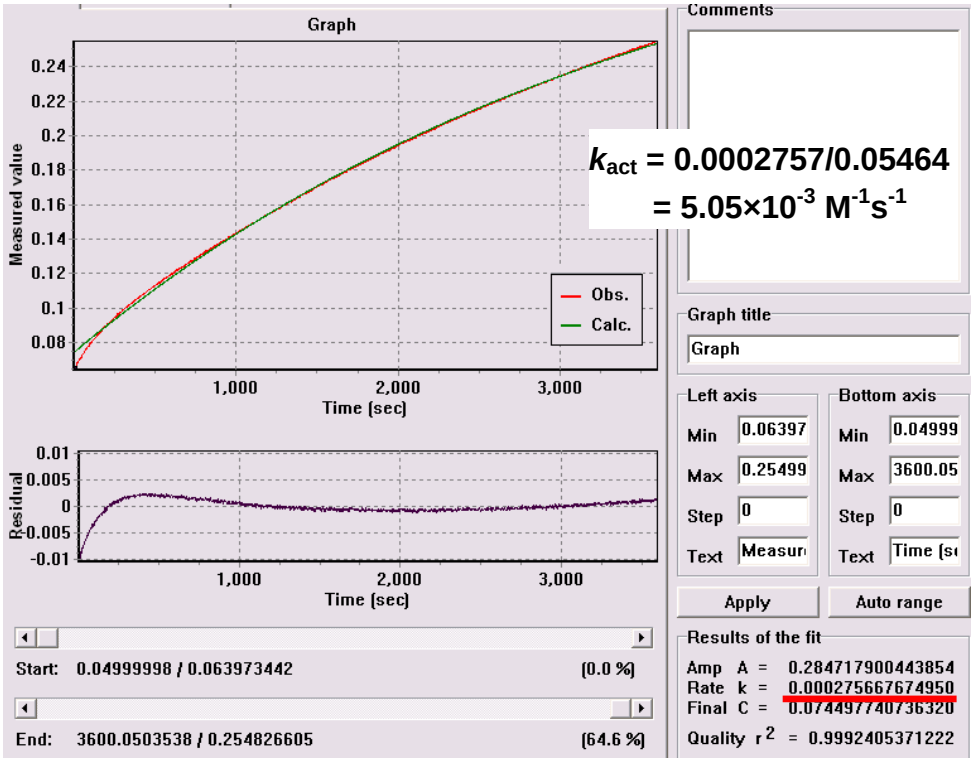

Figure SI10. Measurement of the activation rate constant for $Cu^{(I)}Cl$ species in MeCN at 27 °C. $[CuCl]_o/[bpy]_o/[MBrP]_o$ = 2.73mM/5.44mM/54.64mM.

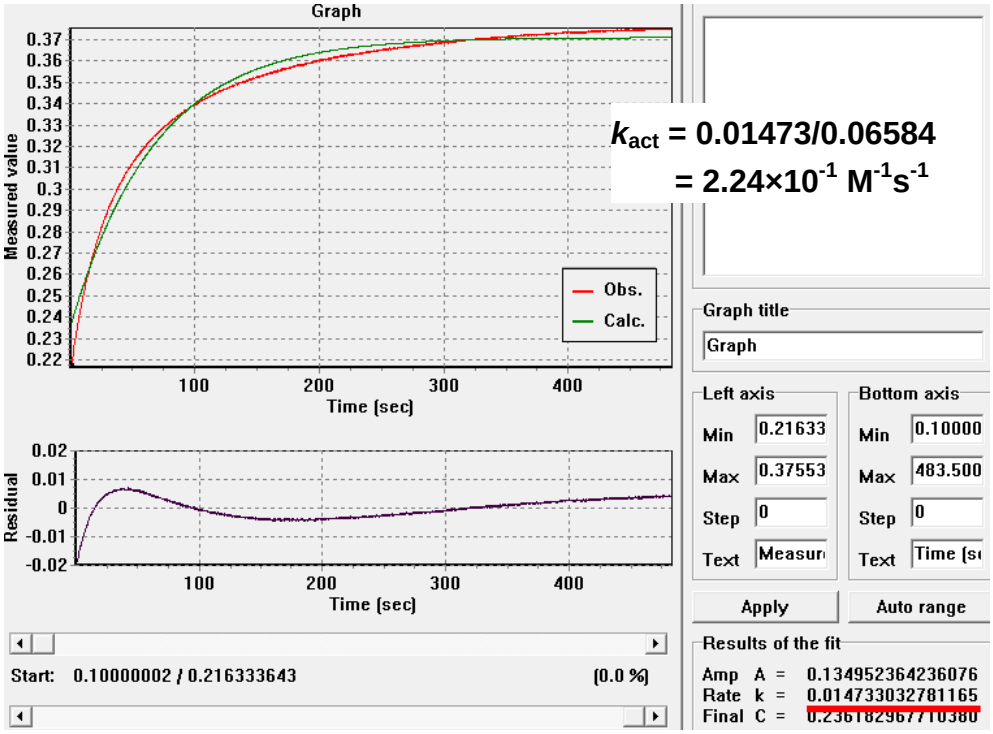

Figure SI11. Measurement of the activation rate constant for $Cu^{(I)}Cl$ species in MeCN at 27 °C. $[CuCl]_o/[bpy]_o/[BrPN]_o$ = 3.31mM/6.65mM/65.84mM.

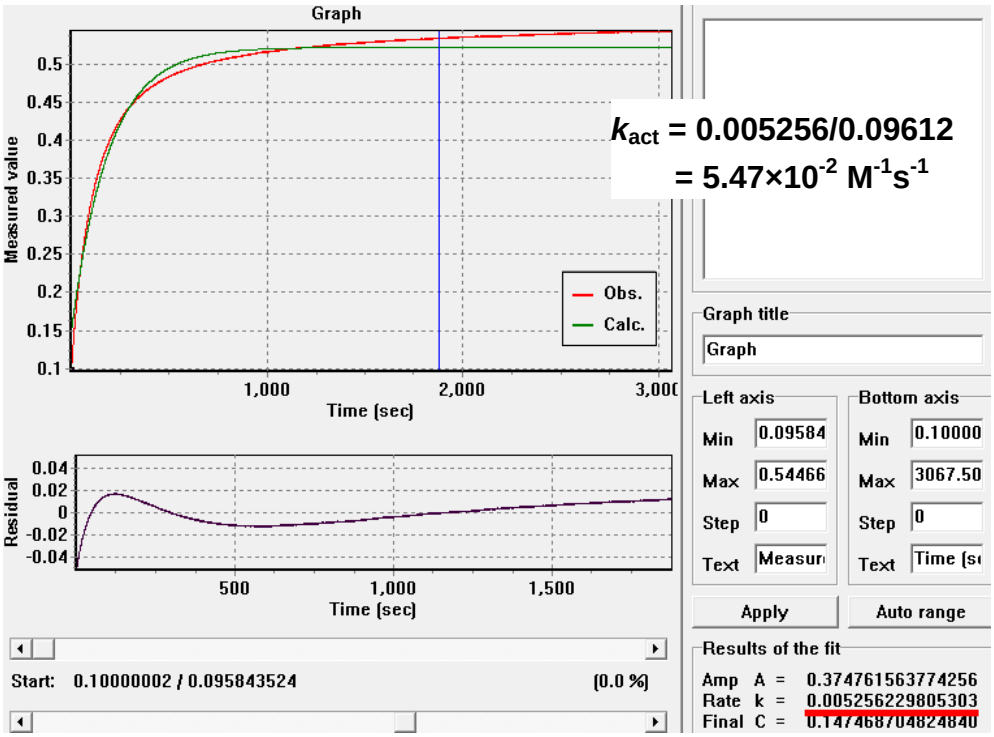

Figure SI12. Measurement of the activation rate constant for $Cu^{(I)}Cl$ species in MeCN at 27 °C. $[CuCl]_o/[bpy]_o/[MBriB]_o$ = 4.68mM/9.40mM/96.12mM.

Measurements of rate constants for an ionic pathway (k_{ionic})

^{1}H NMR spectra were used to follow the increase in concentration of the of alkyl chloride and the decrease of the alkyl bromide in the reactions of $Cl^-{}^+NBu_4$ with the initiators. The slope of the second-order kinetic plots was then utilized for estimation of k_{ionic}.

k_{ionic}: NBu_4Cl/ MBrA

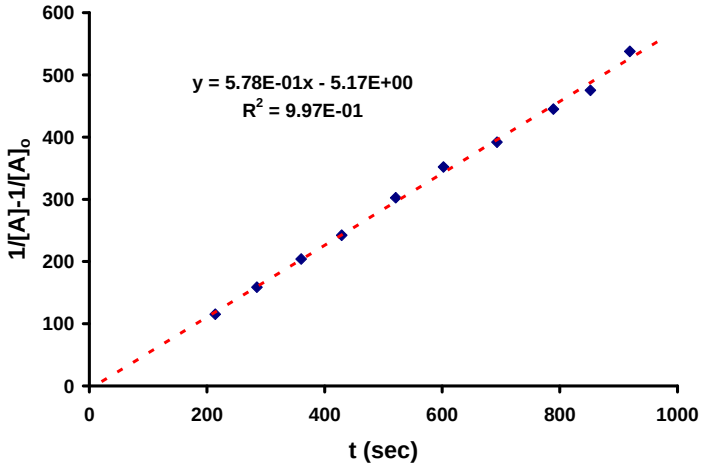

Figure SI13. Measurement of the rate constant for an ionic pathway (k_{ionic}) in MeCN-d_3 at 27 ^{o}C. $[NBu_4Cl]_o = 2.54\times10^{-2}$ M; $[MBrA]_o = 2.54\times10^{-2}$ M, $k_{ionic} = 5.78\times10^{-1}$ $M^{-1}s^{-1}$.

k_{ionic}: NBu_4Cl/ BnBr

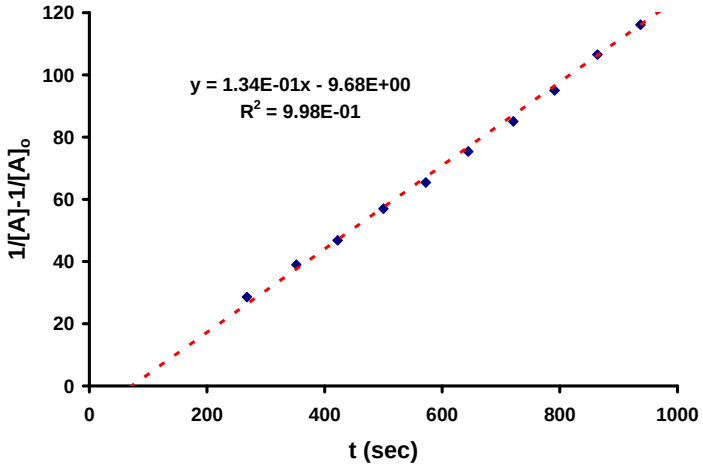

Figure SI14. Measurement of the rate constant for an ionic pathway (k_{ionic}) in MeCN-d_3 at 27 °C. $[NBu_4Cl]_o = 2.02\times10^{-2}$ M; $[BnBr]_o = 2.02\times10^{-2}$ M, $k_{ionic} = 1.34\times10^{-1}$ $M^{-1}s^{-1}$.

k_{ionic}: NBu_4Cl/ BrAN

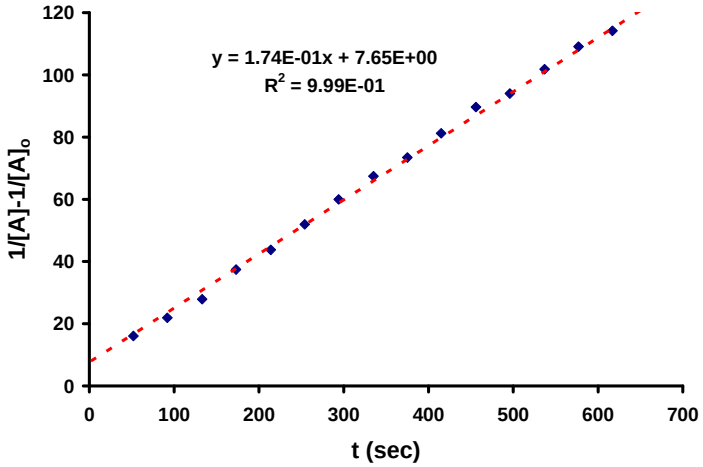

Figure SI15. Measurement of the rate constant for an ionic pathway (k_{ionic}) in MeCN-d_3 at 27 °C. $[NBu_4Cl]_o = 1.16\times10^{-2}$ M; $[BrAN]_o = 1.16\times10^{-2}$ M, $k_{ionic} = 1.74\times10^{-1}$ $M^{-1}s^{-1}$.

k_{ionic}: NBu_4Cl/ MBrP

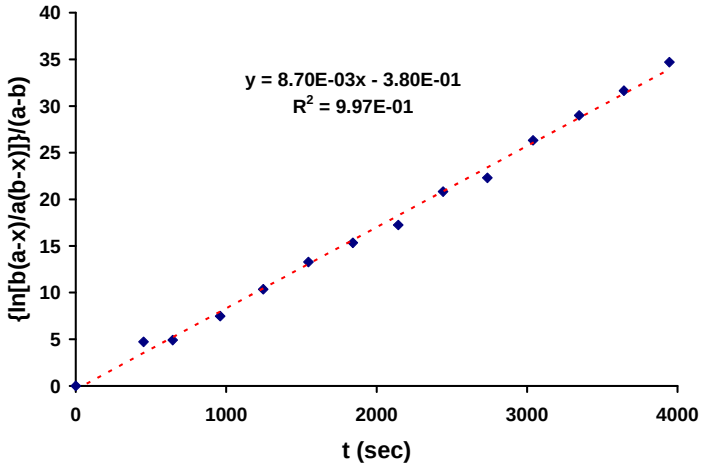

Figure SI16. Measurement of the rate constant for an ionic pathway (k_{ionic}) in MeCN-d_3 at 27 °C. $[NBu_4Cl]_o = 1.56\times10^{-2}$ M; $[MBrP]_o = 2.04\times10^{-2}$ M, $k_{ionic} = 8.70\times10^{-3}$ $M^{-1}s^{-1}$.

k_{ionic}: NBu_4Cl/ PEBr

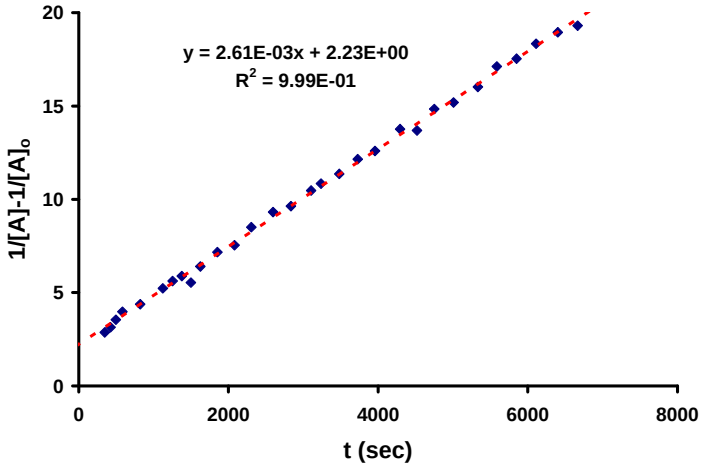

Figure SI17. Measurement of the rate constant for an ionic pathway (k_{ionic}) in MeCN-d_3 at 27 °C. $[NBu_4Cl]_o = 2.05\times10^{-2}$ M; $[PEBr]_o = 2.05\times10^{-2}$ M, $k_{ionic} = 2.61\times10^{-3}$ $M^{-1}s^{-1}$.

k_{ionic}: NBu_4Cl/ BrPN

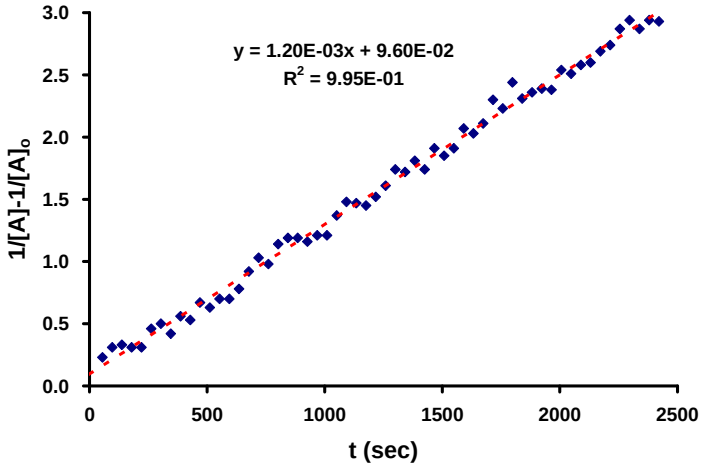

Figure SI18. Measurement of the rate constant for an ionic pathway (k_{ionic}) in MeCN-d_3 at 27 °C. $[NBu_4Cl]_o = 8.09\times10^{-2}$ M; $[BrPN]_o = 8.09\times10^{-2}$ M, $k_{ionic} = 1.20\times10^{-3}$ $M^{-1}s^{-1}$.

k_{ionic}: NBu_4Cl/ MBriB

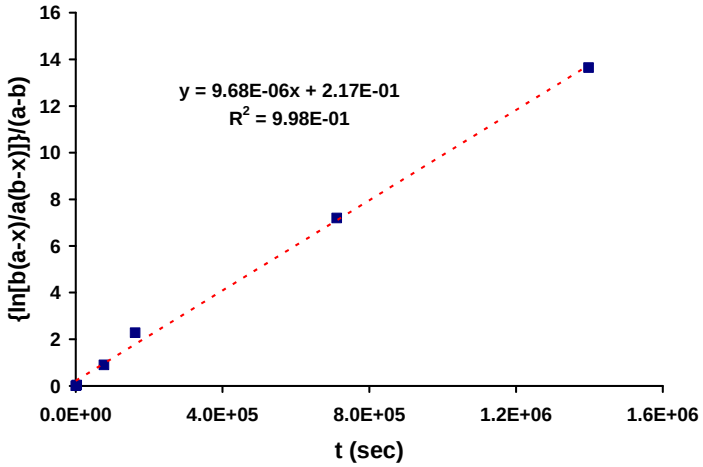

Figure SI19. Measurement of the rate constant for an ionic pathway (k_{ionic}) in MeCN-d_3 at 27 °C. $[NBu_4Cl]_o = 3.09\times10^{-2}$ M; $[MBriB]_o = 2.53\times10^{-2}$ M, $k_{ionic} = 9.68\times10^{-6}$ $M^{-1}s^{-1}$.

k_{ionic} of the initiators with different Cu(II) complexes were also estimated by the slope of the second-order kinetic plots from the reactions of $Cu^{(II)}(L)Cl_2$ (L = TPMA, PMDETA, and bpy) and initiators that were followed by changes in the ^1H NMR spectra.

With $Cu^{(II)}(TPMA)Cl_2$

k_{ionic}: $Cu^{(II)}(TPMA)Cl_2$/ MBrA

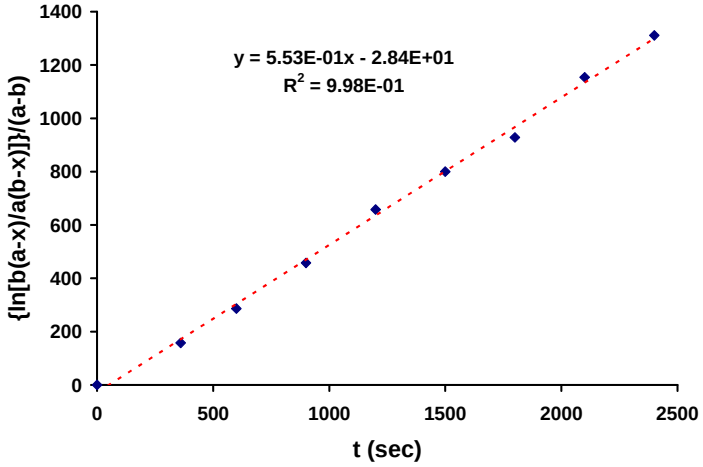

Figure SI20. Measurement of the rate constant for an ionic pathway (k_{ionic}) in MeCN-d_3 at 27 °C. $[Cu^{(II)}(TPMA)Cl_2]_o = 5.83\times10^{-3}$ M; $[MBrA]_o = 4.92\times10^{-3}$ M, $k_{ionic} = 5.53\times10^{-1}$ $M^{-1}s^{-1}$.

k_{ionic}: $Cu^{(II)}(TPMA)Cl_2$/ BnBr

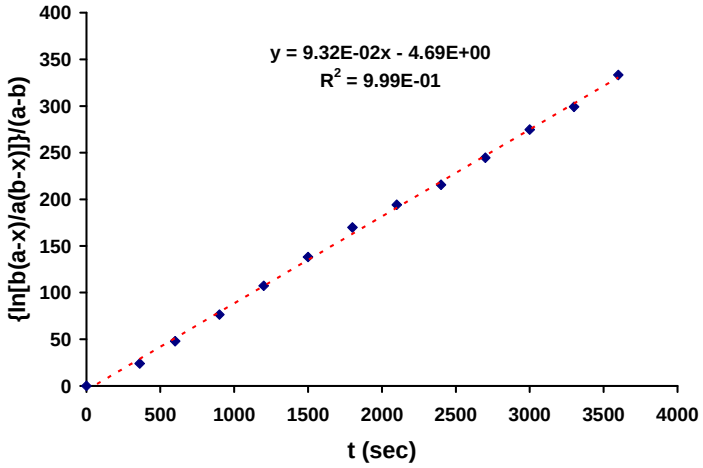

Figure SI21. Measurement of the rate constant for an ionic pathway (k_{ionic}) in MeCN-d_3 at 27 °C. $[Cu^{(II)}(TPMA)Cl_2]_o = 5.83\times10^{-3}$ M; $[BnBr]_o = 6.15\times10^{-3}$ M, $k_{ionic} = 9.32\times10^{-2}$ $M^{-1}s^{-1}$.

k_{ionic}: $Cu^{(II)}(TPMA)Cl_2$/ BrAN

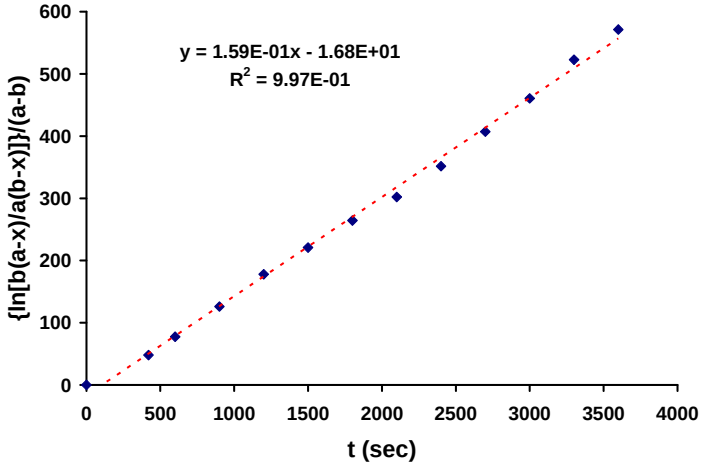

Figure SI22. Measurement of the rate constant for an ionic pathway (k_{ionic}) in MeCN-d_3 at 27 °C. $[Cu^{(II)}(TPMA)Cl_2]_o = 5.83\times10^{-3}$ M; $[BrAN]_o = 7.31\times10^{-3}$ M, $k_{ionic} = 1.59\times10^{-1}$ $M^{-1}s^{-1}$.

k_{ionic}: $Cu^{(II)}(TPMA)Cl_2$/ MBrP

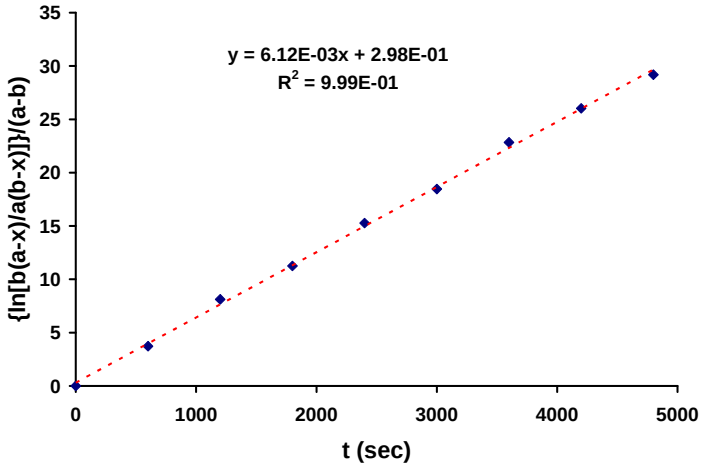

Figure SI23. Measurement of the rate constant for an ionic pathway (k_{ionic}) in MeCN-d_3 at 27 °C. $[Cu^{(II)}(TPMA)Cl_2]_o = 5.83\times10^{-3}$ M; $[MBrP]_o = 5.72\times10^{-3}$ M, $k_{ionic} = 6.12\times10^{-3}$ $M^{-1}s^{-1}$.

k_{ionic}: $Cu^{(II)}(TPMA)Cl_2$/ PEBr

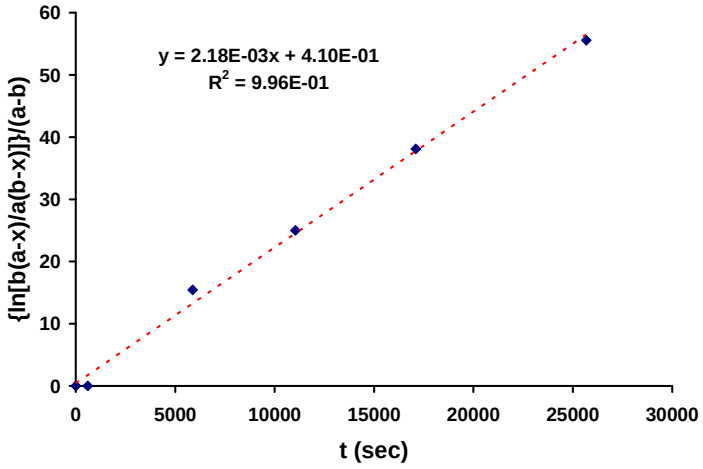

Figure SI24. Measurement of the rate constant for an ionic pathway (k_{ionic}) in MeCN-d_3 at 27 °C. $[Cu^{(II)}(TPMA)Cl_2]_o = 5.83\times10^{-3}$ M; $[PEBr]_o = 5.25\times10^{-3}$ M, $k_{ionic} = 2.18\times10^{-3}$ $M^{-1}s^{-1}$.

k_{ionic}: $Cu^{(II)}(TPMA)Cl_2$/ BrPN

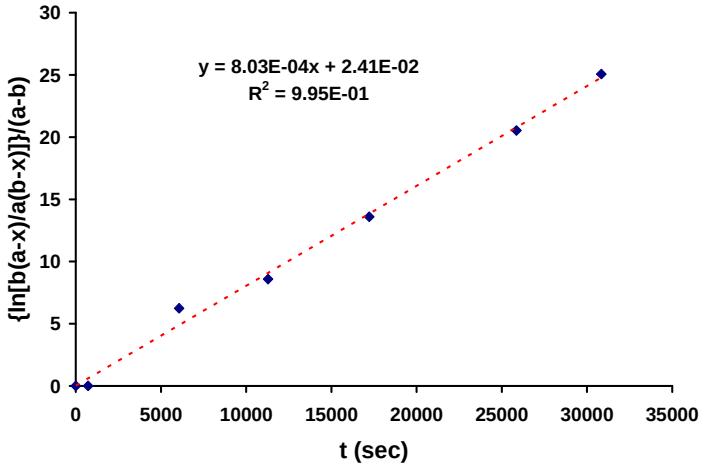

Figure SI25. Measurement of the rate constant for an ionic pathway (k_{ionic}) in MeCN-d_3 at 27 °C. $[Cu^{(II)}(TPMA)Cl_2]_o = 5.83\times10^{-3}$ M; $[BrPN]_o = 5.96\times10^{-3}$ M, $k_{ionic} = 8.03\times10^{-4}$ $M^{-1}s^{-1}$.

k_{ionic}: $Cu^{(II)}(TPMA)Cl_2$/ MBriB

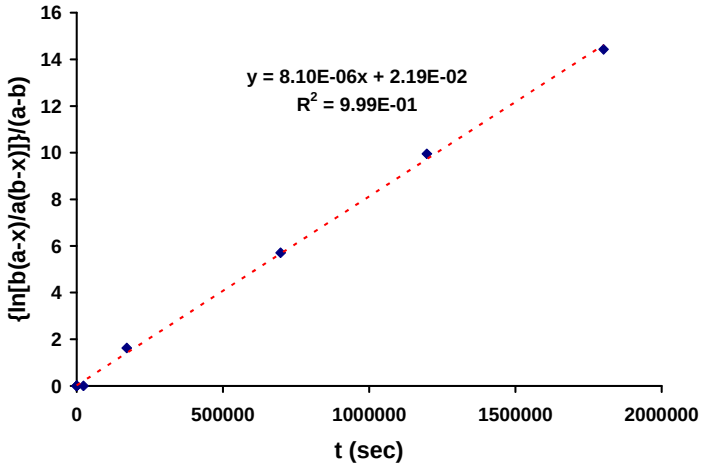

Figure SI26. Measurement of the rate constant for an ionic pathway (k_{ionic}) in MeCN-d_3 at 27 °C. $[Cu^{(II)}(TPMA)Cl_2]_o = 5.83\times10^{-3}$ M; $[MBriB]_o = 4.87\times10^{-3}$ M, $k_{ionic} = 8.10\times10^{-6}$ $M^{-1}s^{-1}$.

With $Cu^{(II)}(PMDETA)Cl_2$

k_{ionic}: $Cu^{(II)}(PMDETA)Cl_2$/ MBrA

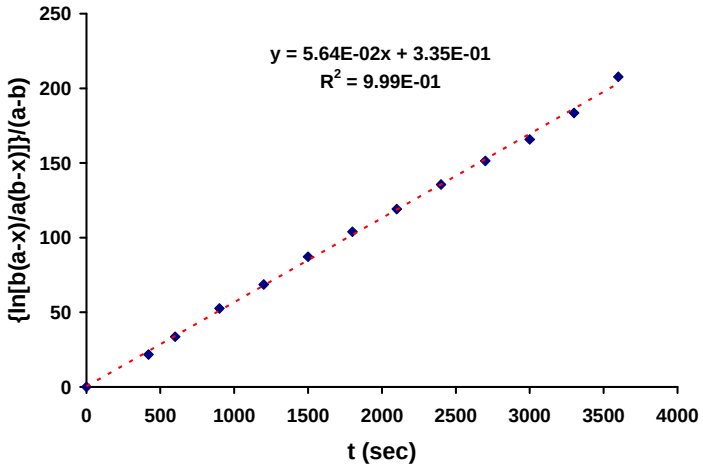

Figure SI27. Measurement of the rate constant for an ionic pathway (k_{ionic}) in MeCN-d_3 at 27 °C. $[Cu^{(II)}(PMDETA)Cl_2]_o = 1.09\times10^{-2}$ M; $[MBrA]_o = 9.47\times10^{-3}$ M, $k_{ionic} = 5.64\times10^{-2}$ $M^{-1}s^{-1}$.

k_{ionic}: $Cu^{(II)}(PMDETA)Cl_2$/ BnBr

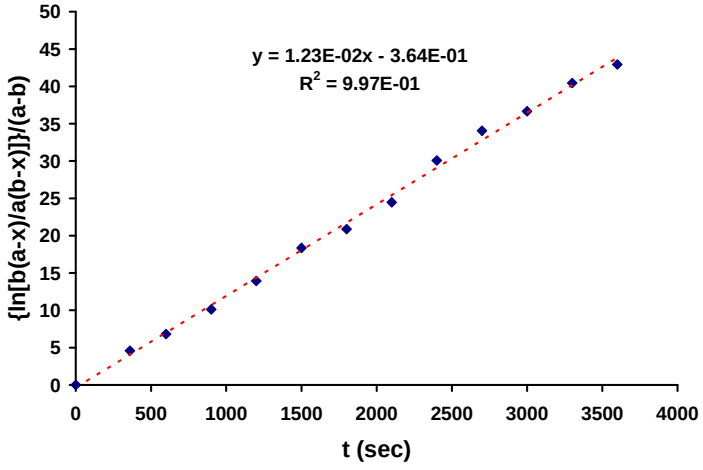

Figure SI28. Measurement of the rate constant for an ionic pathway (k_{ionic}) in MeCN-d_3 at 27 °C. $[Cu^{(II)}(PMDETA)Cl_2]_o = 1.09\times10^{-2}$ M; $[BnBr]_o = 1.18\times10^{-2}$ M, $k_{ionic} = 1.23\times10^{-2}$ $M^{-1}s^{-1}$.

k_{ionic}: $Cu^{(II)}(PMDETA)Cl_2$/ BrAN

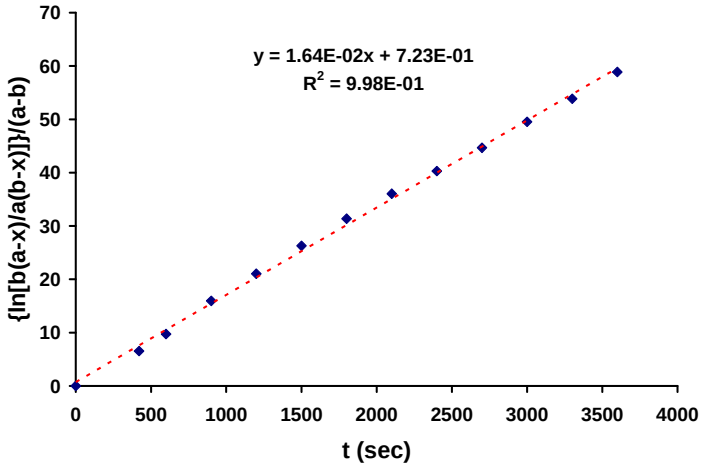

Figure SI29. Measurement of the rate constant for an ionic pathway (k_{ionic}) in MeCN-d_3 at 27 °C. $[Cu^{(II)}(PMDETA)Cl_2]_o = 1.11\times10^{-2}$ M; $[BrAN]_o = 1.08\times10^{-2}$ M, $k_{ionic} = 1.64\times10^{-2}$ $M^{-1}s^{-1}$.

k_{ionic}: $Cu^{(II)}(PMDETA)Cl_2$/ MBrP

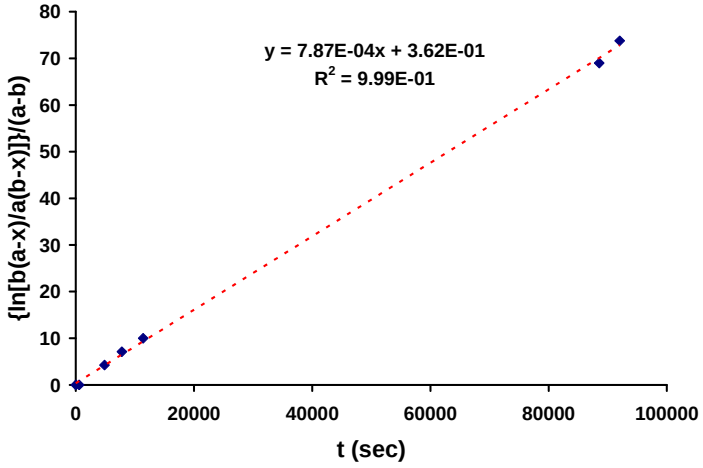

Figure SI30. Measurement of the rate constant for an ionic pathway (k_{ionic}) in MeCN-d_3 at 27 °C. $[Cu^{(II)}(PMDETA)Cl_2]_o = 1.09\times10^{-2}$ M; $[MBrP]_o = 1.10\times10^{-2}$ M, $k_{ionic} = 7.87\times10^{-4}$ $M^{-1}s^{-1}$.

k_{ionic}: $Cu^{(II)}(PMDETA)Cl_2$/ PEBr

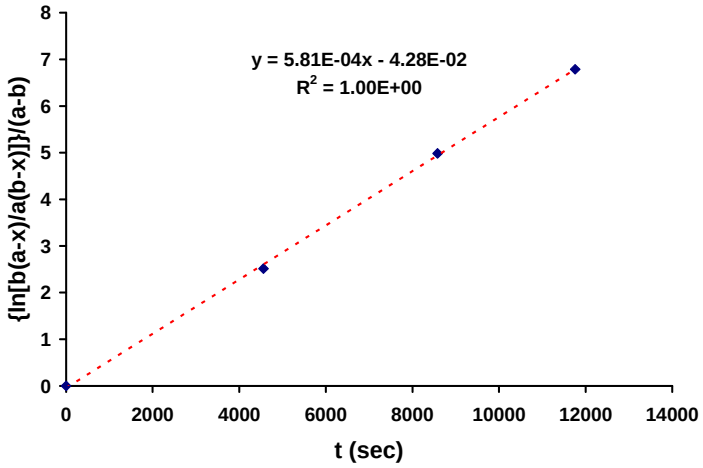

Figure SI31. Measurement of the rate constant for an ionic pathway (k_{ionic}) in MeCN-d_3 at 27 °C. $[Cu^{(II)}(PMDETA)Cl_2]_o = 1.09\times10^{-2}$ M; $[PEBr]_o = 1.01\times10^{-2}$ M, $k_{ionic} = 5.81\times10^{-4}$ $M^{-1}s^{-1}$.

k_{ionic}: $Cu^{(II)}(PMDETA)Cl_2$/ BrPN

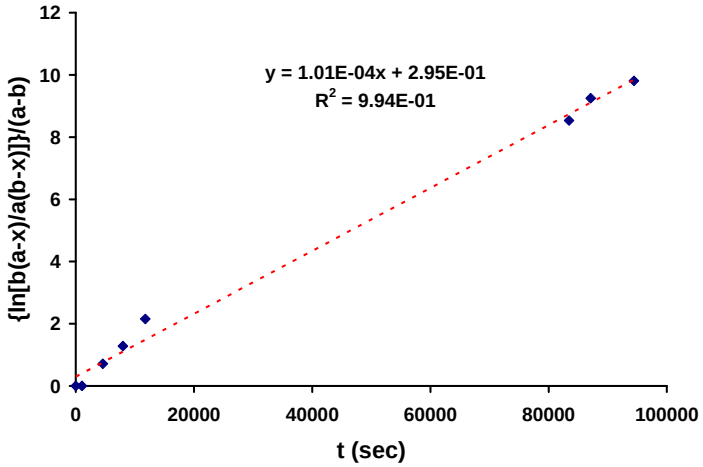

Figure SI32. Measurement of the rate constant for an ionic pathway (k_{ionic}) in MeCN-d_3 at 27 °C. $[Cu^{(II)}(PMDETA)Cl_2]_o = 1.09\times10^{-2}$ M; $[BrPN]_o = 1.15\times10^{-2}$ M, $k_{ionic} = 1.01\times10^{-4}$ $M^{-1}s^{-1}$.

k_{ionic}: $Cu^{(II)}(PMDETA)Cl_2$/ MBriB

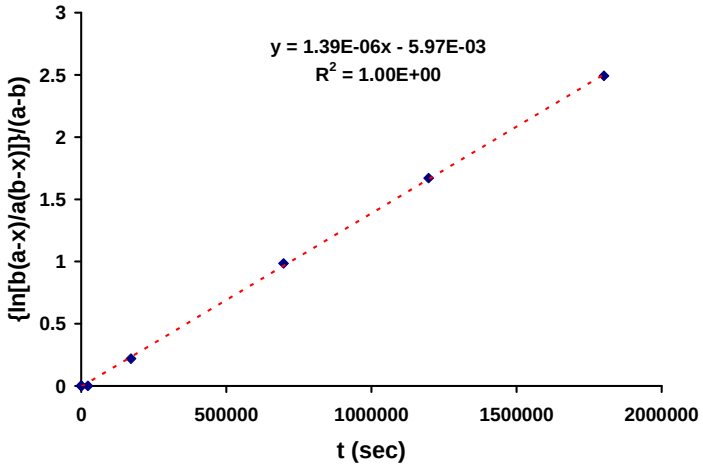

Figure SI33. Measurement of the rate constant for an ionic pathway (k_{ionic}) in MeCN-d_3 at 27 °C. $[Cu^{(II)}(PMDETA)Cl_2]_o = 1.09\times10^{-2}$M; $[MBriB]_o = 9.37\times10^{-3}$M, $k_{ionic} = 1.39\times10^{-6}$ $M^{-1}s^{-1}$.

<u>With $Cu^{(II)}(bpy)_2Cl_2$</u>

k_{ionic}: $Cu^{(II)}(bpy)_2Cl_2$/ MBrA

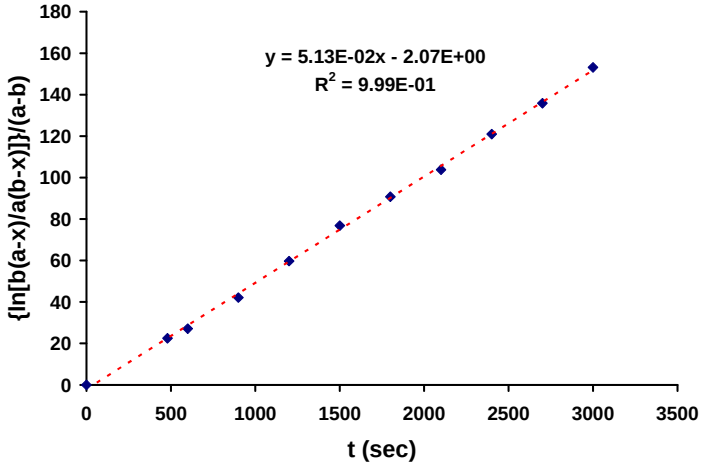

Figure SI34. Measurement of the rate constant for an ionic pathway (k_{ionic}) in MeCN-d_3 at 27 °C. $[Cu^{(II)}(bpy)_2Cl_2]_o = 5.54\times10^{-3}$ M; $[MBrA]_o = 5.03\times10^{-3}$ M, $k_{ionic} = 5.13\times10^{-2}$ $M^{-1}s^{-1}$.

k_{ionic}: $Cu^{(II)}(bpy)_2Cl_2$/ BnBr

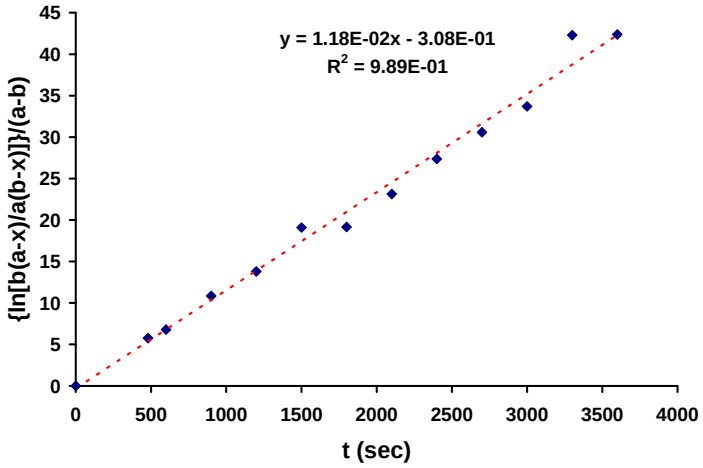

Figure SI35. Measurement of the rate constant for an ionic pathway (k_{ionic}) in MeCN-d_3 at 27 °C. $[Cu^{(II)}(bpy)_2Cl_2]_o = 5.54\times10^{-3}$ M; $[BnBr]_o = 5.62\times10^{-3}$ M, $k_{ionic} = 1.18\times10^{-2}$ $M^{-1}s^{-1}$.

k_{ionic}: $Cu^{(II)}(bpy)_2Cl_2$/ BrAN

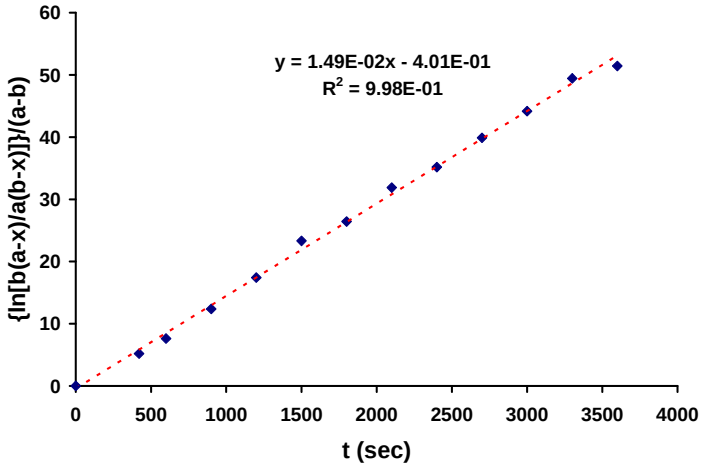

Figure SI36. Measurement of the rate constant for an ionic pathway (k_{ionic}) in MeCN-d_3 at 27 °C. $[Cu^{(II)}(bpy)_2Cl_2]_o = 5.54\times10^{-3}$ M; $[BrAN]_o = 6.41\times10^{-3}$ M, $k_{ionic} = 1.49\times10^{-2}$ $M^{-1}s^{-1}$.

k_{ionic}: $Cu^{(II)}(bpy)_2Cl_2$/ MBrP

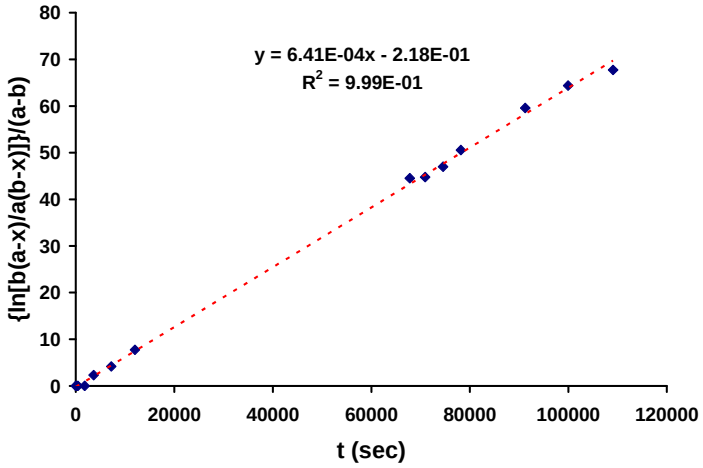

Figure SI37. Measurement of the rate constant for an ionic pathway (k_{ionic}) in MeCN-d_3 at 27 °C. $[Cu^{(II)}(bpy)_2Cl_2]_o = 5.54\times10^{-3}$ M; $[MBrP]_o = 5.76\times10^{-3}$ M, $k_{ionic} = 6.41\times10^{-4}$ $M^{-1}s^{-1}$.

k_{ionic}: $Cu^{(II)}(bpy)_2Cl_2$/ PEBr

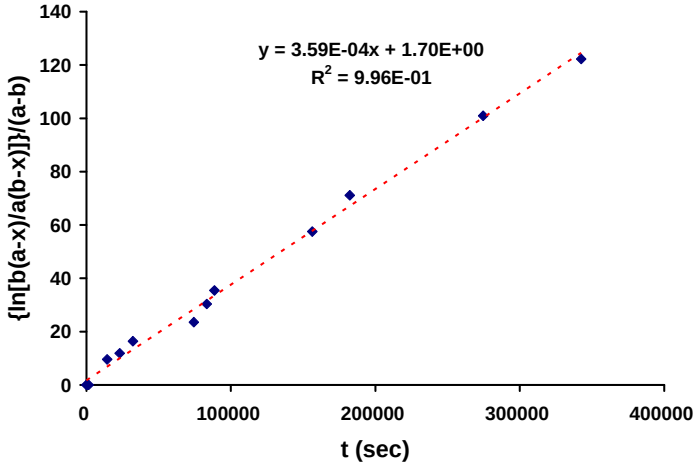

Figure SI38. Measurement of the rate constant for an ionic pathway (k_{ionic}) in MeCN-d_3 at 27 °C. $[Cu^{(II)}(bpy)_2Cl_2]_o = 5.54\times10^{-3}$ M; $[PEBr]_o = 5.20\times10^{-3}$ M, $k_{ionic} = 3.59\times10^{-4}$ $M^{-1}s^{-1}$.

k_{ionic}: $Cu^{(II)}(bpy)_2Cl_2$/ BrPN

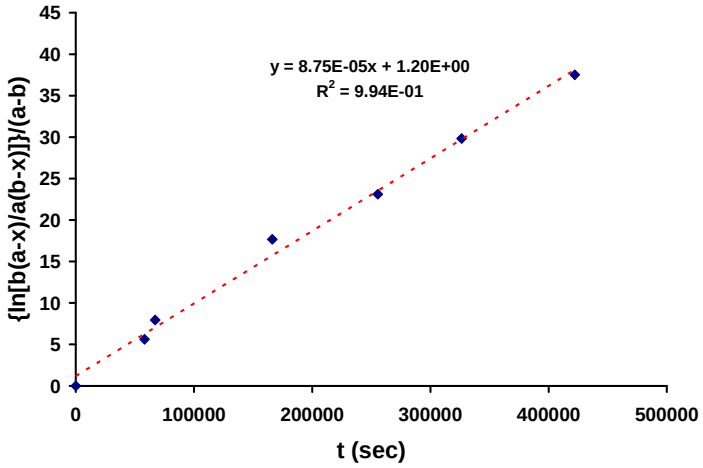

Figure SI39. Measurement of the rate constant for an ionic pathway (k_{ionic}) in MeCN-d_3 at 27 °C. $[Cu^{(II)}(bpy)_2Cl_2]_o = 5.54\times10^{-3}$ M; $[BrPN]_o = 5.74\times10^{-3}$ M, $k_{ionic} = 8.75\times10^{-5}$ $M^{-1}s^{-1}$.

k_{ionic}: $Cu^{(II)}(bpy)_2Cl_2$/ MBriB

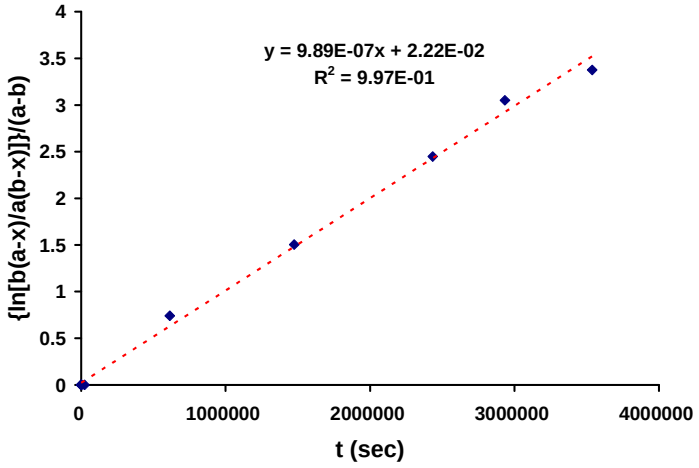

Figure SI40. Measurement of the rate constant for an ionic pathway (k_{ionic}) in MeCN-d_3 at 27 °C. $[Cu^{(II)}(bpy)_2Cl_2]_o = 5.54\times10^{-3}$ M; $[MBriB]_o = 5.31\times10^{-3}$ M, $k_{ionic} = 9.89\times10^{-7}$ $M^{-1}s^{-1}$.

Measurements of rate constants for halogen exchange (k_{HE})

^{1}H NMR spectra were used to follow the increase in concentration of the alkyl chloride and the decrease in alkyl bromide in the reactions of $Cl^{(I)}(L)Cl$ (L = TPMA, PMDETA, and bpy) with the initiators. The slope of the second-order kinetic plots was then utilized for estimation of the value for k_{HE}.

With $Cu^{(I)}$(TPMA)Cl

k_{HE}: $Cu^{(I)}$(TPMA)Cl/ MBrA

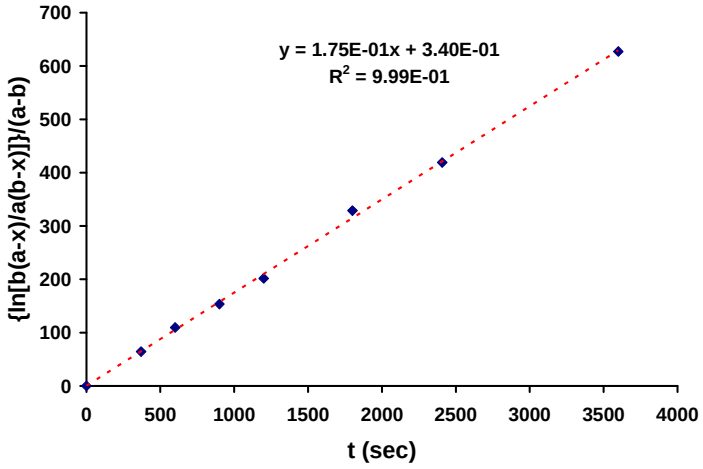

Figure SI41. Measurement of the rate constant for halogen exchange (k_{HE}) in MeCN-d_3 at 27 ^oC. $[Cu^{(I)}(TPMA)Cl]_o = 4.56\times10^{-3}$ M; $[MBrA]_o = 5.11\times10^{-3}$ M, $k_{HE} = 1.75\times10^{-1}$ $M^{-1}s^{-1}$.

k_{HE}: Cu$^{(I)}$(TPMA)Cl/ BnBr

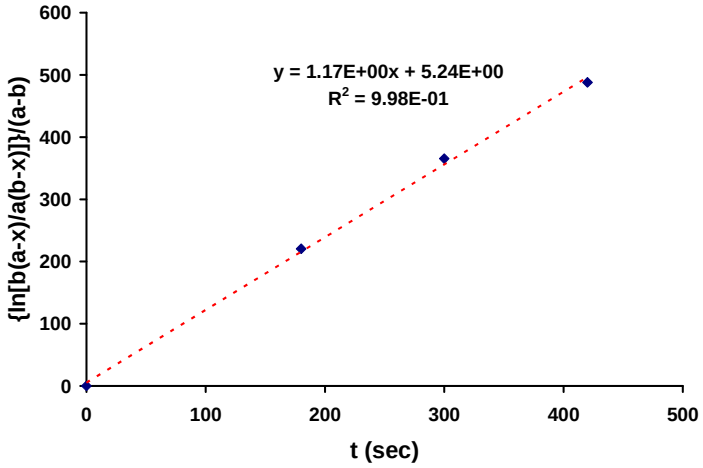

Figure SI42. Measurement of the rate constant for halogen exchange (k_{HE}) in MeCN-d_3 at 27 ^{o}C. $[Cu^{(I)}(TPMA)Cl]_o = 4.60\times10^{-3}$ M; $[BnBr]_o = 5.16\times10^{-3}$ M, $k_{HE} = 1.17$ $M^{-1}s^{-1}$.

k_{HE}: Cu$^{(I)}$(TPMA)Cl/ BrAN

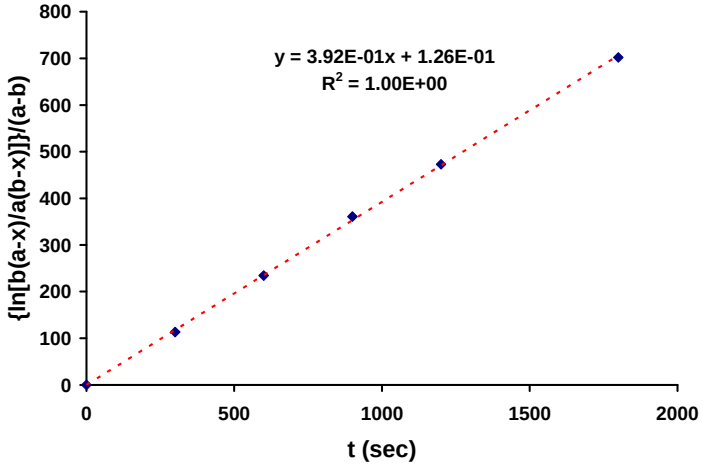

Figure SI43. Measurement of the rate constant for halogen exchange (k_{HE}) in MeCN-d_3 at 27 ^{o}C. $[Cu^{(I)}(TPMA)Cl]_o = 4.63\times10^{-3}$ M; $[BrAN]_o = 4.63\times10^{-3}$ M, $k_{HE} = 3.92\times10^{-1}$ $M^{-1}s^{-1}$.

k_{HE}: Cu$^{(I)}$(TPMA)Cl/ MBrP

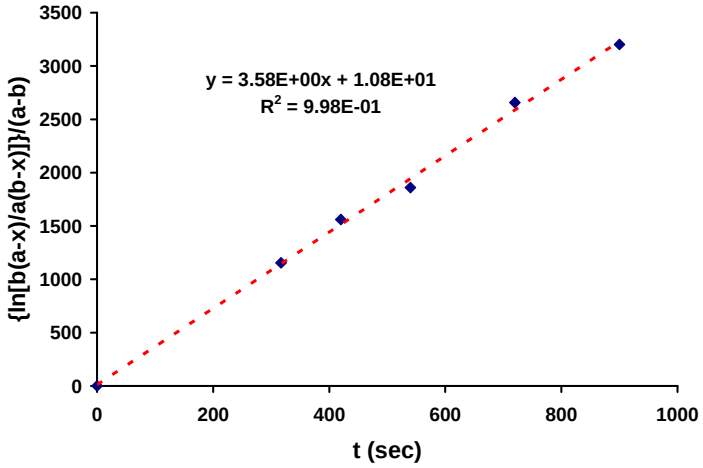

Figure SI44. Measurement of the rate constant for halogen exchange (k_{HE}) in MeCN-d_3 at 27 ^{o}C. $[Cu^{(I)}(TPMA)Cl]_o = 2.58\times10^{-3}$ M; $[MBrP]_o = 3.32\times10^{-3}$ M, $k_{HE} = 3.58$ $M^{-1}s^{-1}$.

k_{HE}: Cu$^{(I)}$(TPMA)Cl/ PEBr

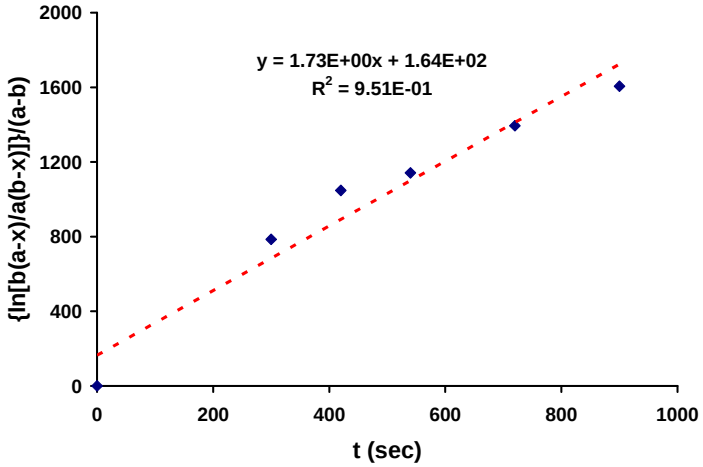

Figure SI45. Measurement of the rate constant for halogen exchange (k_{HE}) in MeCN-d_3 at 27 ^{o}C. $[Cu^{(I)}(TPMA)Cl]_o = 2.62\times10^{-3}$ M; $[PEBr]_o = 2.93\times10^{-3}$ M, $k_{HE} = 1.73$ $M^{-1}s^{-1}$.

k_{HE}: $Cu^{(I)}$(TPMA)Cl/ BrPN

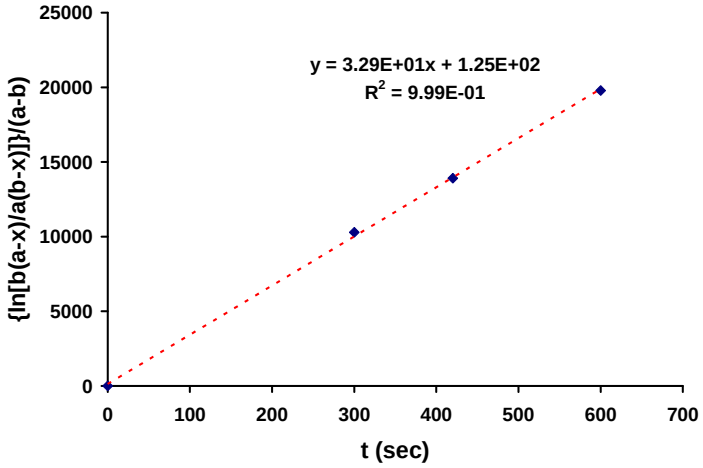

Figure SI46. Measurement of the rate constant for halogen exchange (k_{HE}) in MeCN-d_3 at 27 °C. $[Cu^{(I)}(TPMA)Cl]_o = 4.60\times10^{-3}$ M; $[BrPN]_o = 5.00\times10^{-3}$ M, $k_{HE} = 3.29\times10^{1}M^{-1}s^{-1}$.

k_{HE}: $Cu^{(I)}$(TPMA)Cl/ MBriB

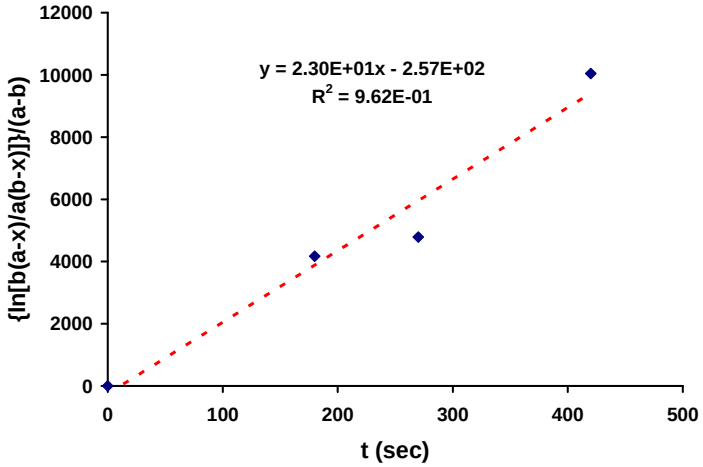

Figure SI47. Measurement of the rate constant for halogen exchange (k_{HE}) in MeCN-d_3 at 27 °C. $[Cu^{(I)}(TPMA)Cl]_o = 1.79\times10^{-3}$ M; $[MBriB]_o = 1.15\times10^{-3}$ M, $k_{HE} = 2.30\times10^{1}M^{-1}s^{-1}$.

With Cu$^{(I)}$(PMDETA)Cl

k_{HE}: Cu$^{(I)}$(PMDETA)Cl/ MBrA

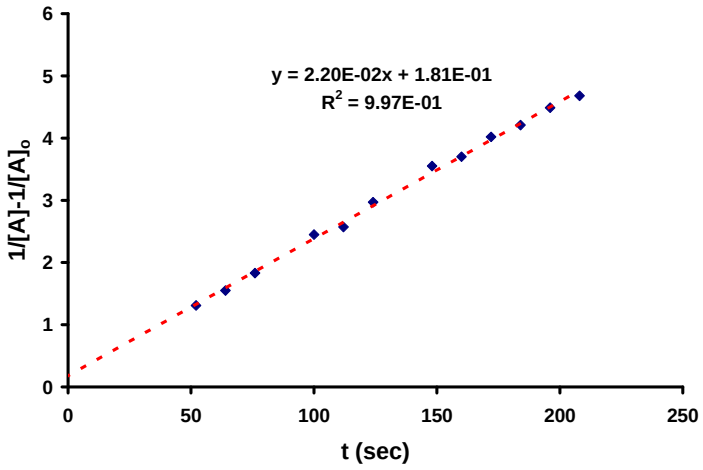

Figure SI48. Measurement of the rate constant for halogen exchange (k_{HE}) in MeCN-d_3 at 27 ^{o}C. $[Cu^{(I)}(PMDETA)Cl]_o = 9.81\times10^{-3}$ M; $[MBrA]_o = 9.81\times10^{-3}$ M, $k_{HE} = 2.20\times10^{-2}M^{-1}s^{-1}$.

k_{HE}: Cu$^{(I)}$(PMDETA)Cl/ BnBr

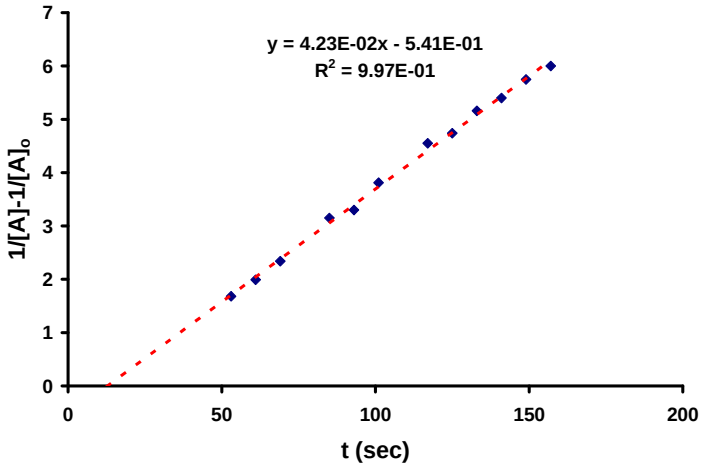

Figure SI49. Measurement of the rate constant for halogen exchange (k_{HE}) in MeCN-d_3 at 27 ^{o}C. $[Cu^{(I)}(PMDETA)Cl]_o = 7.65\times10^{-3}$ M; $[BnBr]_o = 7.65\times10^{-3}$ M, $k_{HE} = 4.23\times10^{-2}M^{-1}s^{-1}$.

k_{HE}: Cu$^{(I)}$(PMDETA)Cl/ BrAN

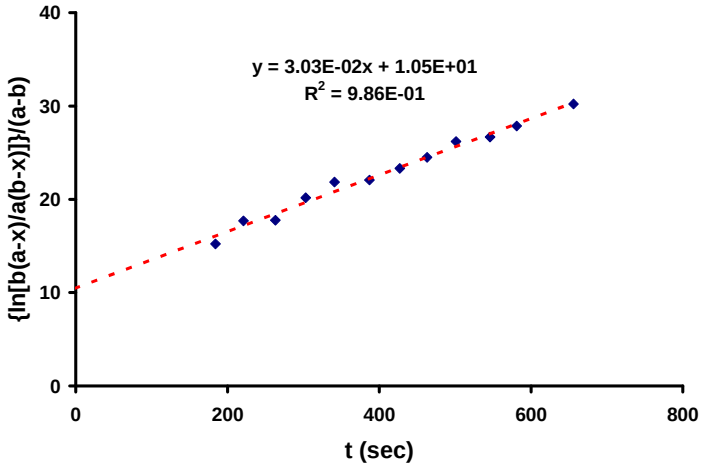

Figure SI50. Measurement of the rate constant for halogen exchange (k_{HE}) in MeCN-d_3 at 27 ^{o}C. $[Cu^{(I)}(PMDETA)Cl]_o = 1.52\times10^{-2}$ M; $[BrAN]_o = 1.88\times10^{-2}$ M, $k_{HE} = 3.03\times10^{-2}$ $M^{-1}s^{-1}$.

k_{HE}: Cu$^{(I)}$(PMDETA)Cl/ MBrP

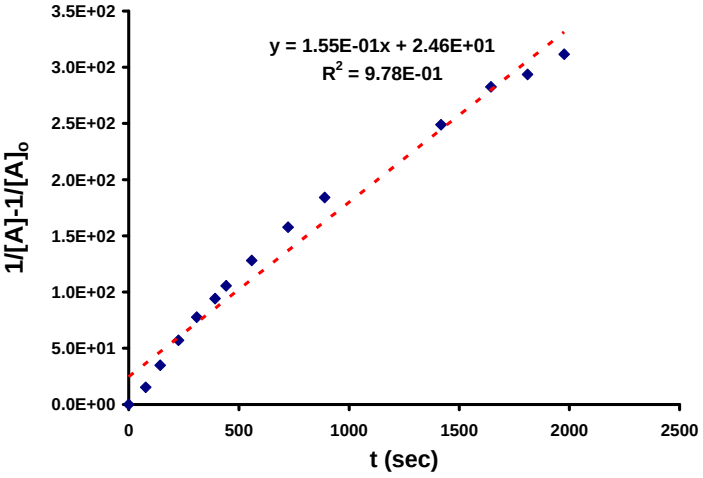

Figure SI51. Measurement of the rate constant for halogen exchange (k_{HE}) in MeCN-d_3 at 27 ^{o}C. $[Cu^{(I)}(PMDETA)Cl]_o = 9.79\times10^{-3}$ M; $[MBrP]_o = 9.79\times10^{-3}$ M, $k_{HE} = 1.55\times10^{-1}$ $M^{-1}s^{-1}$.

k_{HE}: Cu$^{(I)}$(PMDETA)Cl/ PEBr

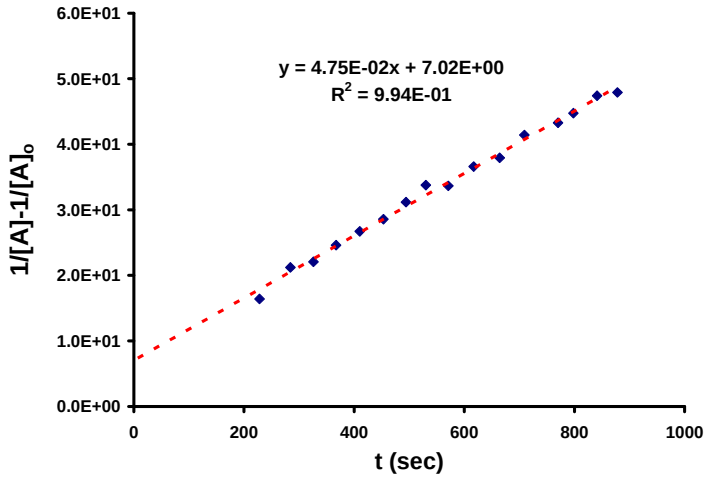

Figure SI52. Measurement of the rate constant for halogen exchange (k_{HE}) in MeCN-d_3 at 27 ^{o}C.

$[Cu^{(I)}(PMDETA)Cl]_o = 1.61\times10^{-2}$ M; $[PEBr]_o = 1.61\times10^{-2}$ M, $k_{HE} = 4.75\times10^{-2}M^{-1}s^{-1}$.

k_{HE}: Cu$^{(I)}$(PMDETA)Cl/ BrPN

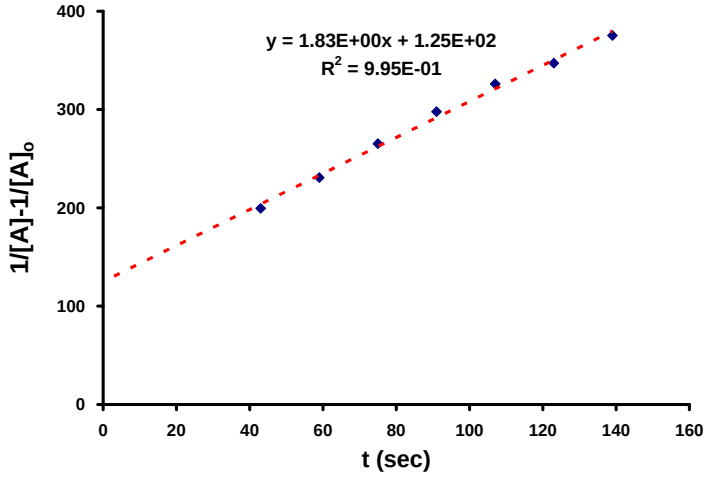

Figure SI53. Measurement of the rate constant for halogen exchange (k_{HE}) in MeCN-d_3 at 27 ^{o}C.

$[Cu^{(I)}(PMDETA)Cl]_o = 6.34\times10^{-3}$ M; $[BrPN]_o = 6.34\times10^{-3}$ M, $k_{HE} = 1.83$ $M^{-1}s^{-1}$.

k_{HE}: $Cu^{(I)}$(PMDETA)Cl/ MBriB

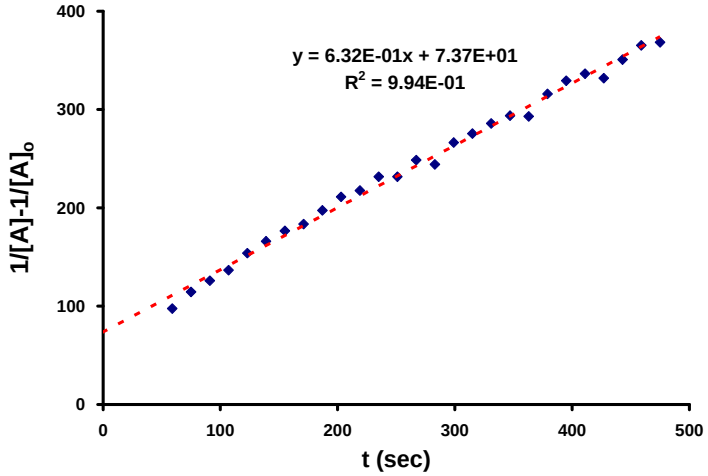

Figure SI54. Measurement of the rate constant for halogen exchange (k_{HE}) in MeCN-d_3 at 27 °C. $[Cu^{(I)}(PMDETA)Cl]_o = 8.96\times10^{-3}$ M; $[MBriB]_o = 8.96\times10^{-3}$ M, $k_{HE} = 6.32\times10^{-1}$ $M^{-1}s^{-1}$.

With $Cu^{(I)}(bpy)_2Cl$

k_{HE}: $Cu^{(I)}(bpy)_2Cl$/ MBrA

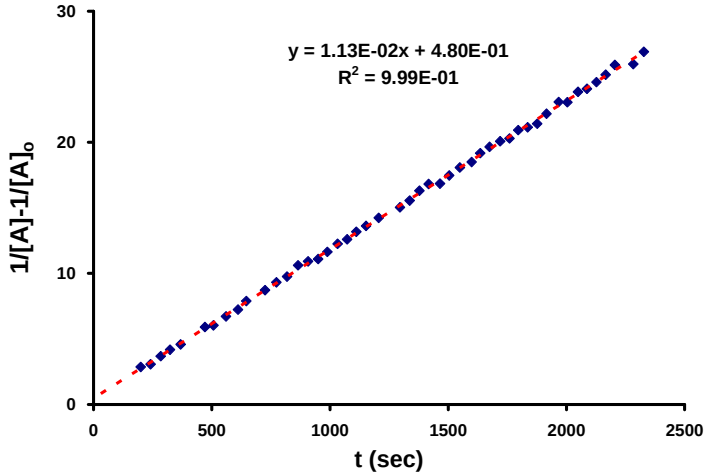

Figure SI55. Measurement of the rate constant for halogen exchange (k_{HE}) in MeCN-d_3 at 27 °C. $[Cu^{(I)}(bpy)_2Cl]_o = 1.98\times10^{-2}$ M; $[MBrA]_o = 1.98\times10^{-2}$ M, $k_{HE} = 1.13\times10^{-2}$ $M^{-1}s^{-1}$.

k_{HE}: $Cu^{(I)}(bpy)_2Cl$/ BnBr

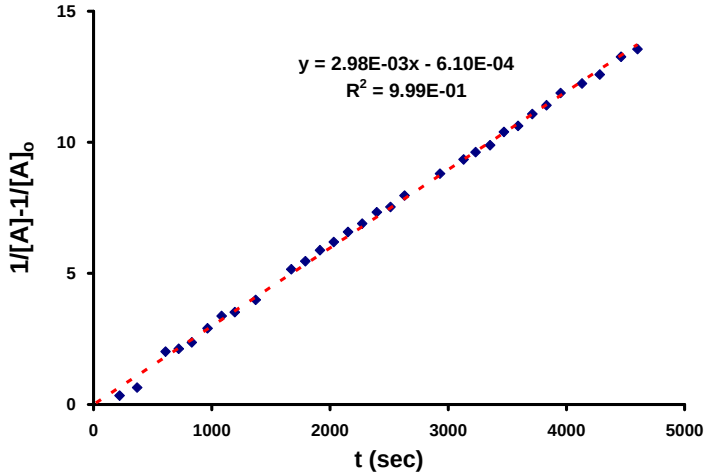

Figure SI56. Measurement of the rate constant for halogen exchange (k_{HE}) in MeCN-d_3 at 27 °C. $[Cu^{(I)}(bpy)_2Cl]_o = 3.00\times10^{-2}$ M; $[BnBr]_o = 3.00\times10^{-2}$ M, $k_{HE} = 2.98\times10^{-3}$ $M^{-1}s^{-1}$.

k_{HE}: $Cu^{(I)}(bpy)_2Cl$/ BrAN

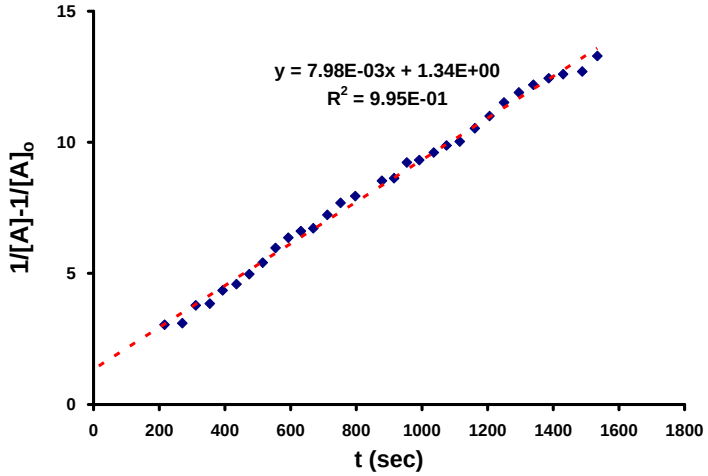

Figure SI57. Measurement of the rate constant for halogen exchange (k_{HE}) in MeCN-d_3 at 27 °C. $[Cu^{(I)}(bpy)_2Cl]_o = 3.00\times10^{-2}$ M; $[BrAN]_o = 3.00\times10^{-2}$ M, $k_{HE} = 7.98\times10^{-3}$ $M^{-1}s^{-1}$.

k_{HE}: $Cu^{(I)}(bpy)_2Cl$/ MBrP

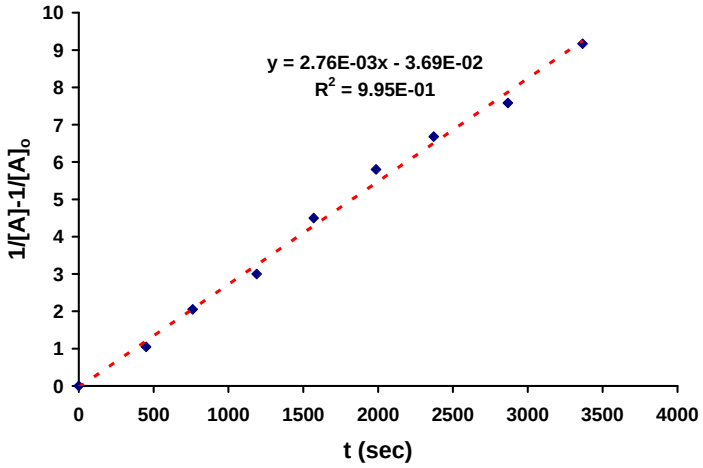

Figure SI58. Measurement of the rate constant for halogen exchange (k_{HE}) in MeCN-d_3 at 27 °C. $[Cu^{(I)}(bpy)_2Cl]_o = 1.90\times10^{-2}$ M; $[MBrP]_o = 1.90\times10^{-2}$ M, $k_{HE} = 2.76\times10^{-3}$ $M^{-1}s^{-1}$.

k_{HE}: $Cu^{(I)}(bpy)_2Cl$/ PEBr

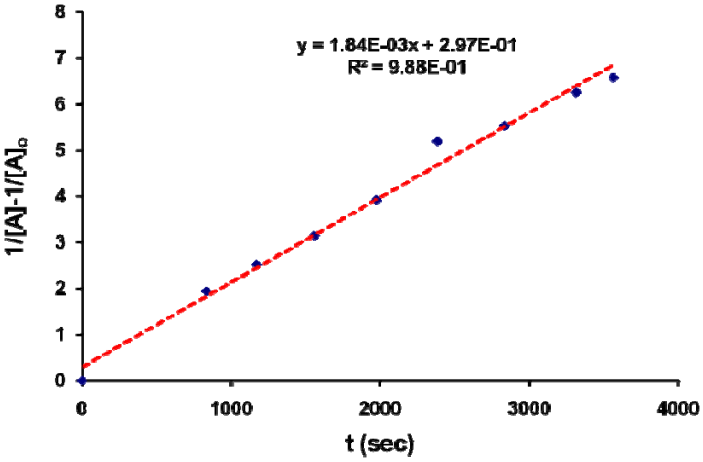

Figure SI59. Measurement of the rate constant for halogen exchange (k_{HE}) in MeCN-d_3 at 27 °C. $[Cu^{(I)}(bpy)_2Cl]_o = 3.01\times10^{-2}$ M; $[PEBr]_o = 3.01\times10^{-2}$ M, $k_{HE} = 1.84\times10^{-3}$ $M^{-1}s^{-1}$.

k_{HE}: $Cu^{(I)}(bpy)_2Cl$/ BrPN

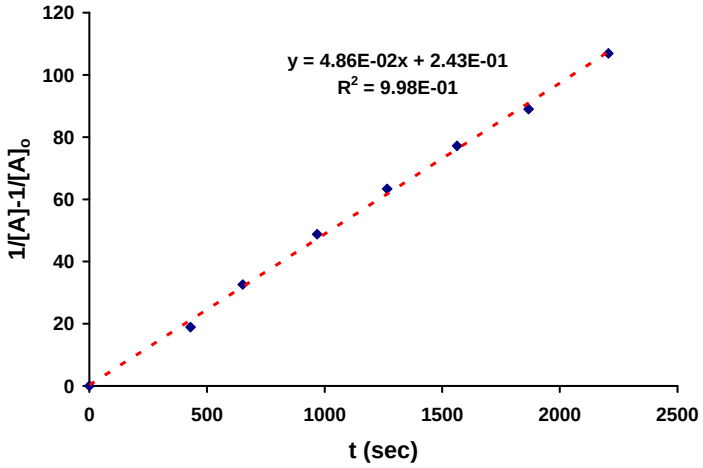

Figure SI60. Measurement of the rate constant for halogen exchange (k_{HE}) in MeCN-d_3 at 27 °C. $[Cu^{(I)}(bpy)_2Cl]_o = 2.03\times10^{-2}$ M; $[BrPN]_o = 2.03\times10^{-2}$ M, $k_{HE} = 4.86\times10^{-2}$ $M^{-1}s^{-1}$.

k_{HE}: $Cu^{(I)}(bpy)_2Cl$/ MBriB

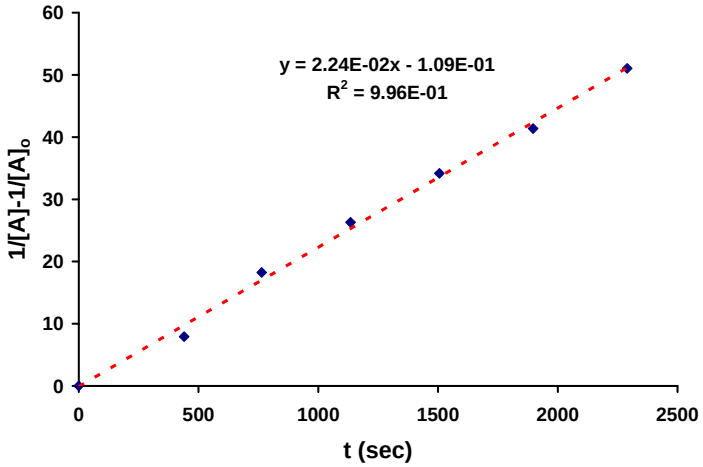

Figure SI61. Measurement of the rate constant for halogen exchange (k_{HE}) in MeCN-d_3 at 27 °C. $[Cu^{(I)}(bpy)_2Cl]_o = 2.01\times10^{-2}$ M; $[MBriB]_o = 2.01\times10^{-2}$ M, $k_{HE} = 2.24\times10^{-2}$ $M^{-1}s^{-1}$.